IEEE Access
Multidisciplinary ⋮ Rapid Review ⋮ Open Access Journal

Received August 1, 2018, accepted September 2, 2018, date of publication September 6, 2018, date of current version October 12, 2018.

Digital Object Identifier 10.1109/ACCESS.2018.2869020

A Variational Bayesian Based Strong Tracking Interpolatory Cubature Kalman Filter for Maneuvering Target Tracking

JIAN WANG, TAO ZHANG, XIANG XU, AND YAO LI
Key Laboratory of Micro-Inertial Instrument and Advanced Navigation Technology, Ministry of Education, Southeast University, Nanjing 210096, China

Corresponding author: Jian Wang (230169708@seu.edu.cn)

This work was supported in part by the National Natural Science Foundation of China under Grant 51375088, in part by the Open Fund of Key Laboratory of Inertial Technology, in part by the Fundamental Research Funds for the Central Universities under Grant 2242015R30031, Grant 2242018K40065, and Grant 2242018K40066, and in part by the Key Laboratory fund of the Ministry of Public Security Based on Large Data Structures under Grant 2015DSJSYS002.

ABSTRACT In tracking a maneuverable target, a proper estimation method with better filtering accuracy, stronger robustness, and faster convergence speed is crucial to the tracking system. The performance of conventional nonlinear Gaussian approximate filters may decline when the target engages in abrupt state changes or the noise covariance matrix is unknown and time-varying. In order to overcome these problems, a new variational Bayesian-based strong tracking interpolatory cubature Kalman filter (VB-STICKF) is deduced in this paper. Gaussian weighted integrals in the nonlinear filter are performed using the interpolatory cubature rule, which has better numerical characteristics for maneuvering target tracking. Moreover, by introducing the strong tracking filter into ICKF, the fading factor is used to modify the predicted error covariance, and the residual sequences are forced to be orthogonal, thus the decreasing performance resulted by the states change and the uncertain process noise could be effectively prevented. Furthermore, the measurement noise can be estimated online by variational Bayesian approach based on the inverse wishart distribution, the robustness of dealing with the uncertain measurement noise is improved. The detailed derivation of VB-STICKF for the general nonlinear models is presented in the paper. A target tracking problem with model uncertainty and time-varying process and measurement noise is utilized to test the performance of the proposed filter, the experimental results of three different scenarios demonstrate the improved filtering performance of the deduced VB-STICKF algorithm.

INDEX TERMS Interpolatory cubature Kalman filter, strong tracking, variational Bayesian, accuracy and robustness.

I. INTRODUCTION

The maneuvering target tracking mainly handles the state estimation problem of the tracking filter to achieve the accurate estimation of the target state, which is the basis for the follow-up tasks, such as target recognition, data fusion, and command decision [1]–[3]. The main means of the target tracking system is the radar, however, with the development of technological means and the complexity and diversity of tracking objects, various target tracking systems and methods, such as radar tracking, infrared tracking, laser tracking, sonar tracking and image tracking, etc, have been developed successively, which further promote the development of the target tracking technology. Maneuvering target tracking has drawn increasing attention because of its widespread application in the fields of the national defense and the civil. In the areas of the military applications, the target tracking is mainly used for long-range warning of battlefields, space target surveillance and early warning, ballistic missile defense, precision guidance, drone mission planning, and low-altitude penetration, etc. For example, the target tracking system use the radar to detect the space target information of the satellites and ballistic missiles, and predict their motion parameters and the warning time. In the field of the civil applications, the target tracking is mainly used for the aviation and traffic control, port vessel navigation and collision avoidance, driverless driving, and electronic medicine, etc.

The research of the target tracking mainly focuses on two aspects [4], one is the modeling of the motion characteristics of the target, numbers of the single models and the multiple models have been proposed, such as the singer model, the current statistical (CS) model, the Jerk model, and the interacting multiple model (IMM), and so on. Another is the research of the filtering tracking algorithm, the target dynamic models and the tracking algorithms have intimate ties, target dynamics during the different phases are substantially different. What a more natural and ideal practice is to develop different models specific for each phase that more fully exploit the inherent characteristics of the portion, however, it is impractical. The applicability of any target dynamic model for a practical problem can hardly be evaluated without referring to the corresponding tracking algorithms, this is because that the established dynamical models can hardly match the maneuvering process endowed with a variety of uncertainties. We can consider solving the problem with the filtering tracking algorithm, so the research of the filtering algorithm with better filtering accuracy and better robustness to resist the model uncertainty and the time-varying process and measurement noise is significant.

The maneuvering target tracking is a representative nonlinear filtering model. An effective approach for nonlinear filtering problem is the Gaussian approximate (GA) filters method [5], [6], which can be achieved by computing the Gaussian approximation to the posterior probability density function (PDF), numbers of GA filtering algorithms using the Bayesian framework have been intensively proposed in recent decades [7], [8]. Since the posteriori distribution is unavailable, which can only be estimated by the prior information of the state and the approximation methods, thus forming some suboptimal nonlinear filters, such as extended Kalman filter (EKF), Gauss-Hermite quadrature filter (GHQF), the cubature Kalman filter (CKF), and the unscented Kalman filter (UKF), etc. However, EKF linearizes the nonlinear models by calculating Jacobian matrix, whose filtering performance will decline when the systems have the complex non-linear character. UKF may load to diverge owing to the fact that the possible negative weight coefficients exist in the integration process [9]. Due to the computational complexity of the GHF with the dimension, GHF is difficult to deal with the high-dimensional systems. Among the Gaussian approximate filters, CKF has higher filtering accuracy, better numerical stability and lower computational complexity than the conventional nonlinear filtering algorithms, such as EKF and UKF. However, it is not sufficiently effective in solving some nonlinear filtering problems [10], [11]. Recently, considerable amount of high-degree nonlinear filtering algorithms have been derived to improve the performance of GA filters. Based on the fifth-degree cubature rule, Jia et al. proposed a fifth-degree CKF in [10]. Different to the orthogonal sampling of the fifth-degree CKF, a fifth-degree non-orthogonal spherical simplex-radial cubature Kalman filter (SSRCKF) algorithm has been deduced in [12]. Other high-degree nonlinear filters, such as the fifth-degree embedded cubature Kalman filter (ECKF) [13], fifth-degree UKF [14], fifth-degree interpolatory cubature Kalman filter (ICKF) [15], fifth-degree cubature quadrature Kalman filter (CQKF) [16], [17], and seventh-degree CKF [18], have been proposed successively, which show better filtering performance than traditional third-degree filters without considering the computational complexity. Since ICKF owns better numerical characteristics than existing fifth-degree GA filters with low computational complexity in [15], the nonlinear filtering algorithm used in the paper is ICKF.

Although ICKF can achieve better estimation accuracy in solving the target tracking problem, the performance may decline, which is caused by a high maneuver or the unknown and time-varying process and measurement noise covariance matrix. In order to overcome these problems, a concept of strong tacking filter (STF) is introduced in [19]–[21], which is a kind of adaptive Kalman filtering algorithms [22]. An adaptive fading factor from STF is added to the filter update, thus the filtering gain matrix could be adaptively adjusted on-line and the residual sequence is forced to be orthogonal, the decreasing performance resulted by model uncertainty could be effectively prevented. However, it isn't allowed to introduce the STF into the ICKF indirectly since that the derivation of STF is based on theoretical frame of EKF, the linear equivalent description of STF to deal with normal nonlinear system was deduced in [23]. An high-degree cubature Kalman filter combined with STF has been derived to overcome the decreasing filtering accuracy of conventional CKF when the states of the target suddenly change in [24]. Liu and Wu [4] introduced the STF algorithm into SSRCKF to handle the nonlinear target tracking problem, which is approximated by the spherical simplex-radial cubature rule.

The decreasing performance resulted by the model uncertainty could be effectively prevented by introducing the STF into nonlinear filters [1], [4], [24], however, the noise statistics may be uncertain in the practical application, which also may affect the filtering accuracy and even lead the filter to diverge. Adaptive Kalman filter methods can be used to deal with this problem, which includes correlation, covariance matching, maximum likelihood and Bayesian methods [25]. The classical Sage-Husa adaptive Kalman filter can't guarantee that noise statistics always converge to the right covariance matrices [26]. The innovation-based adaptive Kalman filter have the drawback of the excessive calculation in the application [27]. Recently, a new variational Bayesian (VB) and Kalman filtering based algorithm is derived and applied to the joint estimation of the measurement noise variances together with the state, however, the algorithm only can solve the linear state space models [28]. Moreover, the variational Bayesian and GA filters based algorithms for the nonlinear systems are deduced in [29]–[32]. Furthermore, By introducing the inverse wishart priors, Huang *et al.* [33] proposed a new adaptive Kalman filter, which shows good filtering performance for the linear model with uncertain process and measurement noise statistics. Meanwhile, many outlier-robust Student's t-based filtering algorithms using the variational Bayesian approaches have been proposed to solve the filtering and smoothing problems of systems with both heavy-tailed process and measurement noises, which provide approximations to posterior filtering and smoothing PDFs.

In this work, we propose a new VB based strong tracking interpolatory cubature Kalman filter (VB-STICKF) to overcome the decreasing filtering performance resulted by the model uncertainty and the time-varying process and measurement noise, which combines ICKF, equivalent STF algorithm and deduced VB based Gaussian approximate filter approach. VB-STICKF is based on the Bayesian framework, under the assumption of the Gaussian distribution and the inverse wishart distribution, Gaussian approximate filter with the fading factor modification is proposed to handle the maneuvering target tracking problem. The main contribution of the paper is that an adaptive filtering algorithm with good filtering accuracy and strong robustness is proposed, we not only consider the condition that the target engages in abrupt state changes, but also take the time-varying process and measurement noises into consideration. By introducing the adaptive fading factor into the equations of time update and measurement update of Gaussian approximate filter, the filtering performance degradation caused by the states change and the time-varying process noise could be effectively prevented, based on the framework of the deduced Gaussian approximate filter based strong tracking filter algorithm, we use VB approach based on the inverse wishart distribution to estimate the measurement noise, which can effectively refine the decreasing filtering performance caused by the time-varying measurement noise.

The rest of the work is given by as follows: The introduction of ICKF algorithm, the deduced VB approach and STF for the nonlinear models are presented in Section II. The proposed VB-STICKF is reported in Section III. Section IV presents experimental results and performance comparisons. Conclusion is summarized in Section V.

II. METHODS

In this section, the fifth-degree ICKF, the deduced VB approach and STF for the nonlinear Gaussian state-space models are respectively described.

A. FIFTH-DEGREE ICKF

Consider a general and discrete expression of nonlinear models:

$$\begin{cases} \boldsymbol{x}_k = f(\boldsymbol{x}_{k-1}) + \boldsymbol{\omega}_{k-1} \\ z_k = h(\boldsymbol{x}_k) + \boldsymbol{v}_k \end{cases} \tag{1}$$

where (1) is the process and the measurement equation, $\boldsymbol{x}_k \in R^n$ denotes the n-dimensional system state vector at time k, $z_k \in R^m$ denotes the m-dimensional measurement vector. $\boldsymbol{\omega}_{k-1}$ and $\boldsymbol{v}_k$ denote zero-mean Gaussian white noise with the covariance matrices $\boldsymbol{Q}_{k-1}$ and $\boldsymbol{R}_k$, respectively. f is the state propagated function and h is the measurement propagated function.

Based on the theoretical framework of Bayesian filtering, the nonlinear filtering problem can be solved by the Gaussian filtering approach, where the filtering distribution is assumed to be approximately Gaussian. Gaussian approximation to posterior density function is widely used to achieve the Gaussian integrals in GA filters. Different filtering algorithms can be obtained by different selections for the Gaussian integral approximations, the multi-dimensional Gaussian integration methods can be described as follow.

$$\boldsymbol{I}[\boldsymbol{g}] = \pi^{-\mathrm{n}/2} \int_{\boldsymbol{R}^n} \boldsymbol{g}(\boldsymbol{x}) \boldsymbol{e}^{-x^T x} d\boldsymbol{x} \tag{2}$$

where $\boldsymbol{I}[\boldsymbol{g}]$ is the general form of multi-dimensional Gaussian integrals, which can be approximated by a $2m+1$ degree fully symmetric interpolatory cubature rule

$$I[\boldsymbol{g}] \approx Q^{(m,n)}[\boldsymbol{g}] = \sum_{\boldsymbol{p} \in P^{(m,n)}} \mathrm{W}_P^{(m,n)} \boldsymbol{g}[\boldsymbol{\lambda}] \tag{3}$$

where $[\boldsymbol{\lambda}]$ is the generator of the sampling point set, $\mathrm{W}_P^{(m,n)}$ are the weighted coefficients of $[\boldsymbol{\lambda}]$, which can be described as

$$\mathrm{W}_P^{(m,n)} = 2^{-K} \sum_{|k| \le m-|p|} \prod_{i=1}^{n} \frac{a_{k_i+p_i}}{\prod_{j=0,\neq p_i}^{k_i+p_i} (\lambda_{p_i}^2 - \lambda_j^2)} \tag{4}$$

where K denotes the number of non-zero entries, $a_0 = 1$, a_i can be given by

$$a_i = \frac{1}{\sqrt{2\pi}} \int_{-\infty}^{+\infty} e^{-x^2/2} \prod_{j=0}^{i-1} (x^2 - \lambda_j^2) dx \quad (i > 0) \tag{5}$$

$P^{(m,n)}$ and the formula $\boldsymbol{g}[\boldsymbol{\lambda}]$ are described as follows

$$\boldsymbol{p}^{(m,n)} = \{(p_1, \ldots, p_n) | \, 0 \le p_n \le \cdots \le p_1, |\boldsymbol{p}| \le m\} \tag{6}$$

$$\boldsymbol{g}[\boldsymbol{\lambda}] = \sum_{q \in \Pi_p} \sum_{s} \boldsymbol{g}[s_1 \lambda_{p_1}, s_2 \lambda_{p_2}, \ldots, s_n \lambda_{p_n}] \tag{7}$$

where Π_p means that we need to compute all distinct permutations of the set of the integers $\boldsymbol{p}$, $s_i = \pm 1$, $\boldsymbol{\lambda} = [\lambda_{p_1}, \lambda_{p_2}, \ldots, \lambda_{p_n}]$, $\lambda_{p_i} \ge 0$, $\lambda_0 = 0$, $\boldsymbol{p} \subset \{0, 1, \ldots, m\}$ and $|\boldsymbol{p}| = \sum_{i=1}^{n} p_i$.

The special fifth-degree interpolatory cubature rule (ICR) has been deduced in [15], when $m = 2$ and $|\boldsymbol{p}| \le 2$, $Q^{(2,n)}$ denotes a new fifth-degree ICR, thus $|\boldsymbol{p}| = 0$, $|\boldsymbol{p}| = 1$, or $|\boldsymbol{p}| = 2$.

$p_i = 0$ and $K = 0$ when $|\boldsymbol{p}| = 0$, the interpolatory cubature point set $\boldsymbol{\lambda} = 0$ and the corresponding weight $W_0^{(2,n)}$ can be obtained as

$$W_0^{(2,n)} = 1 - \frac{n}{\lambda_1^2} + \frac{n(n-1)}{2\lambda_1^4} + \frac{n(3-\lambda_1^2)}{\lambda_1^2 \lambda_2^2} \tag{8}$$

If $|\boldsymbol{p}| = 1$, we get $p_i = 0$ or $p_i = 1$, and only one of them is 1, $K = 1$, the interpolatory cubature point set $\boldsymbol{\lambda}$ and the corresponding weight $W_1^{(2,n)}$ are respectively given by

$$\boldsymbol{\lambda} = \lambda_1 \boldsymbol{e}_i \quad (i = 1, \ldots, n) \tag{9}$$

$$W_1^{(2,n)} = \frac{1}{2}[\frac{1}{\lambda_1^2} + \frac{3-\lambda_1^2}{\lambda_1^2(\lambda_1^2 - \lambda_2^2)} - (n-1)\frac{1}{\lambda_1^4}] \tag{10}$$

where $\boldsymbol{e}_i$ denotes the i-th column of a unit matrix. If $|\boldsymbol{p}| = 2$, then $p_i = p_j = 1$ $(i \neq j)$ or $p_i = 2$. When $p_i = p_j = 1$, then $K = 2$, the interpolatory cubature point sets $\boldsymbol{\lambda} = \lambda_1 \boldsymbol{s}_l^+$ or $\boldsymbol{\lambda} = \lambda_1 \boldsymbol{s}_l^-$, where $\boldsymbol{s}_l^+, \boldsymbol{s}_l^-$ and the corresponding weight $W_2^{(2,n)}$ can be defined as follows

$$\{\boldsymbol{s}_l^+\} = \{e_i + e_j : i < j, i, j = 1, 2, \ldots, n\} \quad (11)$$

$$\{\boldsymbol{s}_l^-\} = \{e_i - e_j : i < j, i, j = 1, 2, \ldots, n\} \quad (12)$$

$$W_2^{(2,n)} = \frac{1}{4\lambda_1^4} \quad (13)$$

If $p_i = 2$, then $K = 1$, the interpolatory cubature point set $\boldsymbol{\lambda}$ and the corresponding weight $W_3^{(2,n)}$ are respectively given by

$$\boldsymbol{\lambda} = \lambda_2 \boldsymbol{e}_i \quad (i = 1, \ldots, n) \quad (14)$$

$$W_3^{(2,n)} = \frac{3 - \lambda_1^2}{2\lambda_2^2(\lambda_2^2 - \lambda_1^2)} \quad (15)$$

The free parameters λ_1 and λ_2 have been calculated in [15], they can be written as follows

$$\begin{cases} \lambda_1 = \sqrt{5 \mp \sqrt{10}} \\ \lambda_2 = \sqrt{5 \pm \sqrt{10}} \end{cases} \quad (16)$$

According to the above analysis, the corresponding interpolatory cubature point sets and the weighted coefficients are respectively obtained as $|\boldsymbol{p}|$ is set as different numerical value, the fifth-degree ICR is concluded as

$$\begin{aligned} Q^{(m,n)}[\boldsymbol{g}] = {} & W_0^{(2,n)} \boldsymbol{g}[\boldsymbol{0}] + W_1^{(2,n)} \sum_{i=1}^{n} [\boldsymbol{g}(\lambda_1 \boldsymbol{e}_i) + \boldsymbol{g}(-\lambda_1 \boldsymbol{e}_i)] \\ & + W_2^{(2,n)} \sum_{i=1}^{n(n-1)/2} [\boldsymbol{g}(\lambda_1 \boldsymbol{s}_i^+) + \boldsymbol{g}(-\lambda_1 \boldsymbol{s}_i^+)) \\ & \qquad + \boldsymbol{g}(\lambda_1 \boldsymbol{s}_i^- + \boldsymbol{g}(-\lambda_1 \boldsymbol{s}_i^-)] \\ & + W_3^{(2,n)} \sum_{i=1}^{n} [\boldsymbol{g}(\lambda_2 \boldsymbol{e}_i) + \boldsymbol{g}(-\lambda_2 \boldsymbol{e}_i)] \end{aligned} \quad (17)$$

We can obtain fifth-degree ICKF algorithm when the fifth-degree ICR is used as Gaussian integration method in GA filter. What's more, the existing fifth-degree CKF is the transformation form of the fifth-degree ICKF by selecting the parameters $\lambda_1 = \sqrt{(n+2)/2}$ and $\lambda_2 = \sqrt{n+2}$.

B. VARIATIONAL BAYESIAN APPROXIMATION ALGORITHM FOR GAUSSIAN APPROXIMATE FILTER

This section deduces a noise adaptive VB based Gaussian approximate filter, which gives one general filtering approach for the nonlinear systems with unknown measurement noise. Based on the Variational Bayesian approximation and the inverse wishart (IW) distribution, the filtering estimation is approximated by the fifth-degree interpolatory cubature integration rule.

Under the Bayesian framework, the posterior probability density $\boldsymbol{p}(x_k | z_{1:k})$ provides a complete statistical description of the state, which can be obtained by combining the filter predictive density $\boldsymbol{p}(x_k | z_{1:k-1})$ and the filter likelihood density $\boldsymbol{p}(z_k | z_{1:k-1})$. We assume that the filtering distribution is approximately Gaussian, the state space model can be reformulated as:

$$\begin{aligned} x_k &\sim \boldsymbol{p}(x_k | x_{k-1}) = \mathrm{N}(f(x_{k-1}), Q_k) \\ z_k &\sim \boldsymbol{p}(z_k | x_k) = \mathrm{N}(h(x_k), R_k) \end{aligned} \quad (18)$$

The purpose of the filtering algorithm is to estimate the joint posterior distribution of the state together with the noise covariance $\boldsymbol{p}(x_k, R_k | z_{1:k})$, the predictive distribution of the measurement noise $\boldsymbol{p}(R_k | R_{k-1})$ is difficult to calculate since that the dynamical model of the noise variance is uncertain, the IW distribution is chosen as the measurement noise predicted distribution in this paper. Suppose that the dynamic models of the state and the noise covariance are mutually independent, the joint posterior probability density function of the state x_{k-1} and the measurement noise covariance R_{k-1} at time $k-1$ can be approximated by the product of a Gaussian distribution with mean $\hat{\boldsymbol{x}}_{k-1|k-1}$ and covariance $\boldsymbol{P}_{k-1|k-1}$ and an IW distribution with parameters $\hat{v}_{k-1|k-1}$ and $\hat{V}_{k-1|k-1}$

$$\begin{aligned} & \boldsymbol{p}(x_{k-1}, R_{k-1} | z_{1:k-1}) \\ & = \boldsymbol{p}(x_{k-1} | z_{1:k-1}) \boldsymbol{p}(R_{k-1} | z_{1:k-1}) \\ & = \mathrm{N}(x_{k-1} | \hat{x}_{k-1|k-1}, P_{k-1|k-1}) \mathrm{IW}(R_{k-1} | \hat{v}_{k-1|k-1}, \hat{V}_{k-1|k-1}) \end{aligned} \quad (19)$$

As the dynamic models of the state and the measurement noise can map the current distributions to the predicted distributions in the same manner, thus, the joint predicted distribution can be formulated as :

$$\begin{aligned} & \boldsymbol{p}(x_k, R_k | z_{1:k-1}) \\ & \quad = \boldsymbol{p}(x_k | z_{1:k-1}) \boldsymbol{p}(R_k | z_{1:k-1}) \\ & \quad = \mathrm{N}(x_k | \hat{x}_{k|k-1}, P_{k|k-1}) \mathrm{IW}(R_k | \hat{v}_{k|k-1}, \hat{V}_{k|k-1}) \end{aligned} \quad (20)$$

where $\hat{x}_{k|k-1}$ and $P_{k|k-1}$ can be calculated by matching the prediction terms of Gaussian approximate filter, the sufficient statistics of the IW distribution at the prediction step can be modeled by as follows

$$\hat{v}_{k|k-1} = \eta(\hat{v}_{k-1|k-1} - m - 1) + m + 1 \quad (21)$$

$$\hat{\boldsymbol{V}}_{k|k-1} = \eta \hat{\boldsymbol{V}}_{k-1|k-1} \quad (22)$$

where η is a real number and $0 < \eta \leq 1$, m is the measurement vector dimension, the parameters of the expected measurement noise $\hat{v}_{k|k}$ and $\hat{\boldsymbol{V}}_{k|k}$ are updated by the factor ρ. Furthermore, the filtering posterior distribution $\boldsymbol{p}(x_k, R_k | z_{1:k})$ at time k can be given by:

$$\begin{aligned} \boldsymbol{p}(x_k, R_k | z_{1:k}) & = \boldsymbol{p}(x_k | z_{1:k}) \boldsymbol{p}(R_k | z_{1:k}) \\ & = \mathrm{N}(x_k | \hat{x}_{k|k}, P_{k|k}) \mathrm{IW}(R_k | \hat{v}_{k|k}, \hat{V}_{k|k}) \end{aligned} \quad (23)$$

The joint posterior distribution can't be obtained by combining the predicted and the likelihood distribution due to the coupled state and measurement noise covariance, to make the computations of the joint posterior tractable, the posterior distribution is approximated by VB approach, which approximates the joint posterior distribution of the state and the noise variances by a factorized form

$$\boldsymbol{p}(x_k, R_k | z_{1:k}) \approx Q_x(x_k) Q_R(R_k) \tag{24}$$

where $Q_x(x_k)$ and $Q_R(R_k)$ are the factorized form distribution, which also can be seen as the yet uncertain probability densities. Based on (23), $Q_x(x_k) = \mathrm{N}(x_k|\hat{x}_{k|k}, P_{k|k})$, $Q_R(R_k) = \mathrm{IW}(R_k|\hat{v}_{k|k}, \hat{V}_{k|k})$, $Q_x(x_k)$ is the Gaussian distribution with mean $\hat{x}_{k|k}$ and covariance $P_{k|k}$, and $Q_R(R_k)$ is the IW distribution with the parameters $\hat{v}_{k|k}$ and $\hat{V}_{k|k}$. $Q_x(x_k)$ and $Q_R(R_k)$ can be formed by minimizing the Kullback-Leibler (KL) divergence between the true distribution and the approximation, the minimum of KL divergence with respect to the probability densities is given by

$$\begin{aligned} Q_x(x_k) &\propto \exp(\int \log \boldsymbol{p}(z_{1:k}, x_k, R_k|z_{1:k-1}) Q_R(R_k) \mathrm{d}R_k) \\ Q_R(R_k) &\propto \exp(\int \log \boldsymbol{p}(z_{1:k}, x_k, R_k|z_{1:k-1}) Q_x(x_k) \mathrm{d}x_k) \end{aligned} \tag{25}$$

The integrals in the exponentials of (25) can be expanded as follows

$$\begin{aligned} &\int \log \boldsymbol{p}(z_{1:k}, x_k, R_k|z_{1:k-1}) Q_R(R_k) \mathrm{d}R_k \\ &= -\frac{1}{2}(z_k - h(x_k))^{\mathrm{T}} \left\langle (R_k)^{-1} \right\rangle_R (z_k - h(x_k)) \\ &\quad -\frac{1}{2}(x_k - \hat{x}_{k|k-1})^{\mathrm{T}} (\boldsymbol{P}_{k|k-1})^{-1} (x_k - \hat{x}_{k|k-1}) + C_1 \\ &\int \log \boldsymbol{p}(z_{1:k}, x_k, R_k|z_{1:k-1}) Q_x(x_k) \mathrm{d}x_k \\ &= -\frac{1}{2}(\hat{v}_{k|k-1} + m + 2) \log |R_k| - \frac{1}{2} tr\{\hat{\boldsymbol{V}}_{k|k-1}(R_k)^{-1}\} \\ &\quad -\frac{1}{2}\left\langle (z_k - h(x_k))^{\mathrm{T}} (R_k)^{-1} (z_k - h(x_k)) \right\rangle_x + C_2 \end{aligned} \tag{26}$$

where $\langle \bullet \rangle_R = \int (\bullet) Q_R(R_k) \mathrm{d}R_k$, $\langle \bullet \rangle_x = \int (\bullet) Q_x(x_k) \mathrm{d}x_k$, and C_1, C_2 are constants. If $Q_R(R_k) = \mathrm{IW}(R_k|\hat{v}_{k|k}, \hat{V}_{k|k})$, we can derive that the expectation in the first equation of (26) can be rewritten as

$$\left\langle (R_k)^{-1} \right\rangle_R = (\hat{v}_{k|k} - m - 1)(\hat{V}_{k|k})^{-1} \tag{27}$$

that is, the equivalent expression of the measurement noise variance matrix can be seen as $R_k = (\hat{v}_{k|k} - m - 1)^{-1}(\hat{V}_{k|k})$. If $Q_x(x_k) = \mathrm{N}(x_k|\hat{x}_{k|k}, P_{k|k})$, the expectation in the second equation of (26) can be reformulated as

$$\begin{aligned} &\left\langle (z_k - h(x_k))^{\mathrm{T}} (R_k)^{-1} (z_k - h(x_k)) \right\rangle_x \\ &\quad = \mathrm{tr}\{\left\langle (z_k - h(x_k))(z_k - h(x_k))^{\mathrm{T}} \right\rangle_x (R_k)^{-1}\} \end{aligned} \tag{28}$$

where the above expectation can be computed by the Gaussian integration methods proposed in [34]. it can be also obtained that $Q_R(R_k)$ is an IW distribution with the following sufficient statistics at the measurement step as follows:

$$v_k = \hat{v}_{k|k-1} + 1 \tag{29}$$

$$\begin{aligned} \hat{\boldsymbol{V}}_{k|k} &= \hat{\boldsymbol{V}}_{k|k-1} + \int (z_k - h(\boldsymbol{x}_k))(z_k - h(\boldsymbol{x}_k))^{\mathrm{T}} \\ &\quad \times N(\boldsymbol{x}_k|\hat{\boldsymbol{x}}_{k|k}, \boldsymbol{P}_{k|k}) \mathrm{d}\boldsymbol{x}_k \end{aligned} \tag{30}$$

The integral in (30) is determined by the selections of the cubature rule for the Gaussian integral approximations, which is carried out by the fifth degree ICR in the paper, Thus, we have

$$\begin{aligned} &\hat{\boldsymbol{V}}_{k|k} \\ &= \hat{\boldsymbol{V}}_{k|k-1} + W_0^{(2,n)}(z_k - h(\boldsymbol{X}_{0i,k|k}))(z_k - h(\boldsymbol{X}_{0i,k|k}))^{\mathrm{T}} \\ &\quad + W_1^{(2,n)} \sum_{j=1}^{2} \sum_{i=1}^{n} (z_k - h(\boldsymbol{X}_{ji,k|k}))(z_k - h(\boldsymbol{X}_{ji,k|k}))^{\mathrm{T}} \\ &\quad + W_2^{(2,n)} \sum_{j=3}^{6} \sum_{i=1}^{n(n-1)/2} (z_k - h(\boldsymbol{X}_{ji,k|k}))(z_k - h(\boldsymbol{X}_{ji,k|k}))^{\mathrm{T}} \\ &\quad + W_3^{(2,n)} \sum_{j=7}^{8} \sum_{i=1}^{n} (z_k - h(\boldsymbol{X}_{ji,k|k}))(z_k - h(\boldsymbol{X}_{ji,k|k}))^{\mathrm{T}} \end{aligned} \tag{31}$$

where $\boldsymbol{X}_{ji,k|k}$ is the sampling fifth-degree ICR points with mean $\hat{\boldsymbol{x}}_{k|k}$ and covariance $\boldsymbol{P}_{k|k}$, by substituting the expectations (27) and (28) into (26), a general VB adaptive Gaussian approximation filter algorithm for the nonlinear models can be obtained as follows by matching the parameters in left and right hand sides of (25)

1) Compute the parameters of the predicted distribution:

$$\begin{aligned} \hat{\boldsymbol{x}}_{k|k-1} &= \mathrm{E}(\boldsymbol{x}_k | z_{1:k-1}) \\ &= \int \boldsymbol{f}(\boldsymbol{x}_{k-1}) \mathrm{N}(\boldsymbol{x}_{k-1}|\hat{\boldsymbol{x}}_{k-1|k-1}, \\ &\quad \boldsymbol{P}_{k-1|k-1}) \mathrm{d}\boldsymbol{x}_{k-1} \end{aligned} \tag{32}$$

$$\begin{aligned} \boldsymbol{P}_{k|k-1} &= \mathrm{E}((\boldsymbol{x}_k - \hat{\boldsymbol{x}}_{k|k-1})(\boldsymbol{x}_k - \hat{\boldsymbol{x}}_{k|k-1})^T \Big| z_{1:k-1}) \\ &= \int \boldsymbol{f}(\boldsymbol{x}_{k-1}) \boldsymbol{f}^T(\boldsymbol{x}_{k-1}) \times \mathrm{N}(\boldsymbol{x}_{k-1}|\hat{\boldsymbol{x}}_{k-1|k-1}, \\ &\quad \boldsymbol{P}_{k-1|k-1}) \times \mathrm{d}\boldsymbol{x}_{k-1} - \hat{\boldsymbol{x}}_{k|k-1}\hat{\boldsymbol{x}}_{k|k-1}^T + \boldsymbol{Q}_{k-1} \end{aligned} \tag{33}$$

$$\hat{v}_{k|k-1} = \eta(\hat{v}_{k-1|k-1} - m - 1) + m + 1 \tag{34}$$

$$\hat{\boldsymbol{V}}_{k|k-1} = \eta \hat{\boldsymbol{V}}_{k-1|k-1} \tag{35}$$

2) Compute the Variational Measurement Update as follows: set $\hat{\boldsymbol{x}}_{k|k}^{(0)} = \hat{\boldsymbol{x}}_{k|k-1}$, $\boldsymbol{P}_{k|k}^{(0)} = \boldsymbol{P}_{k|k-1}$, $v_k = \hat{v}_{k|k-1} + 1$, $\hat{\boldsymbol{V}}_{k|k}^{(0)} = \hat{\boldsymbol{V}}_{k|k-1}$, and compute the following:

$$\hat{z}_{k|k-1} = \int \boldsymbol{h}(\boldsymbol{x}_k) \times \mathrm{N}(\boldsymbol{x}_k|\hat{\boldsymbol{x}}_{k|k-1}, \boldsymbol{P}_{k|k-1}) \mathrm{d}\boldsymbol{x}_k \tag{36}$$

$$\begin{aligned} \boldsymbol{P}_{zz,k|k-1} &= \int \boldsymbol{h}(\boldsymbol{x}_k) \boldsymbol{h}^T(\boldsymbol{x}_k) \times \mathrm{N}(\boldsymbol{x}_k|\hat{\boldsymbol{x}}_{k|k-1}, \\ &\quad \times \boldsymbol{P}_{k|k-1}) \mathrm{d}\boldsymbol{x}_k - \hat{z}_{k|k-1}\hat{z}_{k|k-1}^T \end{aligned} \tag{37}$$

$$\begin{aligned} \boldsymbol{P}_{xz,k|k-1} &= \int \boldsymbol{x}_k \boldsymbol{h}^T(\boldsymbol{x}_k) \times \mathrm{N}(\boldsymbol{x}_k|\hat{\boldsymbol{x}}_{k|k-1}, \boldsymbol{P}_{k|k-1}) \mathrm{d}\boldsymbol{x}_k \\ &\quad - \hat{\boldsymbol{x}}_{k|k-1}\hat{z}_{k|k-1} \end{aligned} \tag{38}$$

Iterate the following update equations, say N, steps are set as $i = 0, \ldots, N$:

$$P^{(i+1)}_{zz,k|k-1} = P_{zz,k|k-1} + (v_k - m - 1)^{-1}\hat{V}^{(i)}_{k|k} \tag{39}$$

$$K^{(i+1)} = P_{xz,k|k-1}(P^{(i+1)}_{zz,k|k-1})^{-1} \tag{40}$$

$$\hat{x}^{(i+1)}_{k|k} = \hat{x}_{k|k-1} + K^{(i+1)}(z_k - \hat{z}_{k|k-1}) \tag{41}$$

$$P^{(i+1)}_{k|k} = P_{k|k-1} - K^{(i+1)}P^{(i+1)}_{zz,k|k-1}[K^{(i+1)}]^T \tag{42}$$

$$\hat{V}^{(i+1)}_{k|k} = \hat{V}_{k|k-1} + \int (z_k - h(x_k))(z_k - h(x_k))^{\mathrm{T}} \times \mathrm{N}(x_k|\hat{x}^{(i)}_{k|k}, P^{(i)}_{k|k})\mathrm{d}x_k \tag{43}$$

Set $\hat{V}_{k|k} = \hat{V}^{(N)}_{k|k}, \hat{x}_{k|k} = \hat{x}^{(N)}_{k|k}, P_{k|k} = P^{(N)}_{k|k}$.

We can see that the prediction step of the algorithm consists of the Gaussian approximation filter prediction and the heuristic prediction, the variances are increased by the factor η, the update step can be used as a fixed point iteration with the obtained expected noise covariance. All the multidimensional integrals in the filtering algorithm can be computed by Gaussian integral approximations based on the selection of different integral rules. The integral in (43) can be performed exploiting the appropriate integral rules, it is important to note that the mean and the covariance of the sampling points are $\hat{x}_{k|k}$ and $P_{k|k}$ at time k, respectively.

C. STRONG TRACKING FILTER ALGORITHM FOR NONLINEAR MODELS

EKF is a most widely used nonlinear filtering algorithm with the advantages of simpler engineering implementation and lower computational account. However, EKF has strict requirements on the system model, the strong nonlinearities and the uncertainties of the system model will result in a decrease in the accuracy of the state estimation, and even cause the filter to diverge.

It has been proven that the residual sequences are the mutually uncorrelated Gaussian white noise sequences when the theoretical model is exactly matched to the actual model [35]. Inspired by this theory, Zhou *et al.* [36] proposed a STF algorithm to improve the robustness of EKF when the system is with the model uncertainty. A general structure of the STF algorithm for the nonlinear system can be given by :

$$\hat{x}_{k|k} = \hat{x}_{k|k-1} + K_k\gamma_k \tag{44}$$

where $\gamma_k = z_{k|k} - h\left(\hat{x}_{k|k-1}\right)$ is the theoretical value of the residual sequence at time k, $\hat{x}_{k|k-1} = f(\hat{x}_{k-1|k-1})$ is one-step state prediction, a sufficient condition for the above filter with the strong tracking filter characteristics is to adjust the filtering gain K_k adaptively, making it satisfy the following two conditions simultaneously:

$$\begin{cases} \mathrm{E}[(\hat{x}_{k|k} - \hat{x}_{k|k-1})(\hat{x}_{k|k} - \hat{x}_{k|k-1})^{\mathrm{T}}] = \min \\ \mathrm{E}[\gamma_{k+j}(\gamma_k)^{\mathrm{T}}] = 0, \quad k = 1, 2, 3 \ldots;\ j = 1, 2, \ldots \end{cases} \tag{45}$$

where the first equation in (45) is the performance indicator of EKF, which means achieving the optimal estimation with the least mean square error, the second equation in (45) reveals that residual sequences should remain orthogonal to each other in different times, the above two equations constitute the orthogonality principle.

The orthogonality principle has obvious physical significance, when the established model does not exactly match the actual system, the residual sequences are forced to be orthogonal by adjusting the filtering gain K_k adaptively, which has uncorrelated Gaussian white noise-like properties. It means that all valid information in the residual sequence have been extracted by the filter, so that the STF algorithm have the ability to track the system state with high precision when the system model is uncertain. In this way, the algorithm can be given by as follows

$$\hat{x}_{k|k-1} = f(\hat{x}_{k-1|k-1}) \tag{46}$$

$$P_{k|k-1} = \lambda_k F_{k/k-1}P_{k-1/k-1}F^{\mathrm{T}}_{k/k-1} + Q_{k-1} \tag{47}$$

$$\hat{z}_{k|k-1} = h\left(\hat{x}_{k|k-1}\right) \tag{48}$$

$$K_k = P_{k|k-1}H^{\mathrm{T}}_k(H_kP_{k|k-1}H^{\mathrm{T}}_k + R_k)^{-1} \tag{49}$$

$$\hat{x}_{k|k} = \hat{x}_{k|k-1} + K_k(z_{k|k} - \hat{z}_{k|k-1}) \tag{50}$$

$$P_{k|k} = (I - K_kH_k)P_{k|k-1} \tag{51}$$

where λ_k is the fading factor, $F_{k/k-1}$ and H_k are the process matrix and measure matrix, respectively, they are calculated by the first-order Taylor series expansion.

$$F_{k/k-1} = \frac{\partial f(x_{k-1})}{\partial x_{k-1}}|x_{k-1} = \hat{x}_{\mathrm{k-1|k-1}} \tag{52}$$

$$H_k = \frac{\partial h(x_k)}{\partial x_k}|x_k = \hat{x}_{\mathrm{k|k-1}} \tag{53}$$

Then, λ_k can be obtained by the following equations

$$\lambda_k = \max(1, \frac{tr[N_k]}{tr[M_k]}) \tag{54}$$

$$N_k = V_k - H_kQ_{k-1}H^{\mathrm{T}}_k - \beta R_k \tag{55}$$

$$M_k = H_kF_{k/k-1}P_{k-1/k-1}F^{\mathrm{T}}_{k/k-1}H^{\mathrm{T}}_k - \beta R_k \tag{56}$$

$$V_k = \begin{cases} \varepsilon_1\varepsilon_1^{\mathrm{T}}, & k = 1 \\ \dfrac{\rho V_{k-1} + \varepsilon_1\varepsilon_1^{\mathrm{T}}}{1+\rho}, & k \geq 2 \end{cases} \tag{57}$$

$$\varepsilon_k = z_{k|k} - \hat{z}_{k|k-1} \tag{58}$$

where $tr[\bullet]$ is the trace operation, $0 < \rho \leq 1$ is the forgetting factor, $\beta \geq 1$ is the softening factor.

By introducing the STF into the EKF and modifying the predicted state error covariance matrix by an adaptive fading factor, thus the filtering gain could be adaptively adjusted on-line, the residual sequence is forced to be orthogonal, which has effectively refined the poor filtering performance caused by the uncertainty factors. Relying on the fading factor, the STF algorithm makes full use of the effective information in the residual sequence and shows better robustness to resist the uncertainties of the system model. When there is no large model mismatch, the fading factor can be automatically taken as 1, just like EKF, it does not affect the estimation accuracy of the system state.

However, the STF algorithm still need to compute the Jacobian matrix since that the derivation of STF is based on theoretical frame of EKF, it isn't allowed to introduce the STF into the Gaussian approximate filter indirectly, Wang *et al.* [23] has provided the linear equivalent description of STF and could deal with normal nonlinear system, $\boldsymbol{H}_k, \boldsymbol{N}_k$ and $\boldsymbol{M}_k$ can be defined as follows

$$\boldsymbol{H}_k = (\boldsymbol{P}_{xz,k|k-1})^{\mathrm{T}}[(\boldsymbol{P}_{k|k-1})^{-1}]^{\mathrm{T}} \tag{59}$$

$$\boldsymbol{N}_k = \boldsymbol{V}_k - (\boldsymbol{P}_{xz,k|k-1})^{\mathrm{T}}[(\boldsymbol{P}_{k|k-1})^{-1}]^{\mathrm{T}}\boldsymbol{Q}_{k-1}(\boldsymbol{P}_{k|k-1})^{-1} \times \boldsymbol{P}_{xz,k|k-1} - \beta \boldsymbol{R}_k \tag{60}$$

$$\boldsymbol{M}_k = \boldsymbol{P}_{zz,k|k-1} + \boldsymbol{N}_k - \boldsymbol{V}_k + (\beta - 1)\boldsymbol{R}_k \tag{61}$$

where $\boldsymbol{P}_{k|k-1}$, $\boldsymbol{P}_{xz,k|k-1}$ and $\boldsymbol{P}_{zz,k|k-1}$ are one-step predicted state error covariance matrix, the predicted measurement covariance matrix and the measurement cross-covariance matrix before introducing STF into Gaussian approximate filter, respectively, which can be approximated by the fifth-degree ICR mentioned in the paper. An adaptive fading factor λ_k for the normal nonlinear system can be obtained by substituting (60) and (61) for (55) and (56), the subsequent derivations for the normal nonlinear models are similar to STF algorithm according to (46)-(51), it is worth mentioning that the nonlinear filtering problem is solved by the Gaussian approximate filters method, the multidimensional Gaussian-weighted integrals are approximated by the fifth-degree ICR in the paper, the specific application of STF in the proposed VB-STICKF algorithm is shown in Section III.

III. VARIATIONAL BAYESIAN BASED ADAPTIVE STRONG TRACKING INTERPOLATORY CUBATURE KALMAN FILTER

In this section, a VB based adaptive strong tracking ICKF (VB-STICKF) is proposed for a target tracking problem with uncertain models and time-varying process and measurement noise, which can modify the prediction state error covariance by a fading factor, and the time-varying measurement noise can be estimated by VB approximation. VB-STICKF algorithm can be formulated by the following steps:

1) Initialization: The initial state is assumed to be Gaussian distribution with $\hat{\boldsymbol{x}}_{0|0}$ and $\boldsymbol{P}_{0|0}$

$$\begin{cases} \hat{\boldsymbol{x}}_{0|0} = \mathrm{E}(\boldsymbol{x}_{0|0}) \\ \boldsymbol{P}_{0|0} = \mathrm{E}((\hat{\boldsymbol{x}}_{0|0} - \boldsymbol{x}_{0|0})(\hat{\boldsymbol{x}}_{0|0} - \boldsymbol{x}_{0|0})^T) \end{cases} \tag{62}$$

The corresponding weights of the fifth-degree ICKF $W_0^{(2,n)}$, $W_1^{(2,n)}$, $W_2^{(2,n)}$, $W_3^{(2,n)}$ with free parameters λ_1 and λ_2 are calculated through the analyses of the derived fifth-degree ICKF, and the interpolatory cubature point sets $\boldsymbol{\xi}_l$ can be achieved based on ICR ($l = 1, 2, \ldots, 2n^2 + 2n + 1$).

2) Time update: Assume that the state estimation $\hat{\boldsymbol{x}}_{k-1|k-1}$ and the corresponding covariance $\boldsymbol{P}_{k-1|k-1}$ at time $k-1$ are known, that is, the posterior distribution $\boldsymbol{p}(x_{k1}\, z_{1:k-1}) = \mathrm{N}(x_{k-1}|\hat{x}_{k-1|k-1}, P_{k-1|k-1})$ is known. Factorize covariance matrix $\boldsymbol{P}_{k-1|k-1}$ using Cholesky decomposition

$$P_{k-1|k-1} = \boldsymbol{S}_{k-1|k-1}\boldsymbol{S}_{k-1|k-1}^T \tag{63}$$

Evaluate the fifth-degree interpolatory cubature points ($l = 1, 2, \ldots, 2n^2 + 2n + 1$)

$$\boldsymbol{X}_{l,k-1|k-1} = \boldsymbol{S}_{k-1|k-1}\boldsymbol{\xi}_l + \hat{\boldsymbol{x}}_{k-1|k-1} \tag{64}$$

Evaluate cubature points through the state equation in (1) ($l = 1, 2, \ldots, 2n^2 + 2n + 1$)

$$\boldsymbol{X}^*_{l,k-1|k-1} = f(\boldsymbol{X}_{l,k-1|k-1}) \tag{65}$$

Compute the predicted state

$$\hat{\boldsymbol{x}}_{k|k-1} = \mathrm{W}_0^{(2,\mathrm{n})}\boldsymbol{X}^*_{l,k-1|k-1} + \mathrm{W}_1^{(2,\mathrm{n})}\sum_{l=2}^{2n+1}\boldsymbol{X}^*_{l,k-1|k-1} + \mathrm{W}_2^{(2,\mathrm{n})}\sum_{l=2n+2}^{2n^2+1}\boldsymbol{X}^*_{l,k-1|k-1} + \mathrm{W}_3^{(2,\mathrm{n})}\sum_{l=2n^2+2}^{2n^2+2n+1}\boldsymbol{X}^*_{l,k-1|k-1} \tag{66}$$

Estimate the one-step predicted error covariance without introducing the fading factor

$$\begin{aligned}\boldsymbol{P}_{k|k-1} = {} & W_0^{(2,n)}\boldsymbol{X}^*_{l,k-1|k-1}(\boldsymbol{X}^*_{1,k-1|k-1})^T + W_1^{(2,n)}\sum_{l=2}^{2n+1}\boldsymbol{X}^*_{l,k-1|k-1}(\boldsymbol{X}^*_{1,k-1|k-1})^T \\ & + W_2^{(2,n)}\sum_{l=2n+2}^{2n^2+1}\boldsymbol{X}^*_{l,k-1|k-1}(\boldsymbol{X}^*_{1,k-1|k-1})^T + W_3^{(2,n)}\sum_{l=2n^2+2}^{2n^2+2n+1}\boldsymbol{X}^*_{l,k-1|k-1}(\boldsymbol{X}^*_{1,k-1|k-1})^T \\ & - \hat{\boldsymbol{x}}_{k|k-1}\hat{\boldsymbol{x}}^T_{k|k-1} + \boldsymbol{Q}_{k-1}\end{aligned} \tag{67}$$

Compute the parameters of the predicted measurement noise,which can be given by as follows:

$$\begin{cases} \hat{v}_{k|k-1} = \eta(\hat{v}_{k-1|k-1} - m - 1) + m + 1 \\ \hat{\boldsymbol{V}}_{k|k-1} = \eta\hat{\boldsymbol{V}}_{k-1|k-1} \end{cases} \tag{68}$$

where η is a real number and $0 < \eta \leq 1$, m is the measurement vector dimension.

3) Measurement update: We set $\hat{\boldsymbol{x}}^{(0)}_{k|k} = \hat{\boldsymbol{x}}_{k|k-1}$, $\boldsymbol{P}^{(0)}_{k|k} = \boldsymbol{P}_{k|k-1}$, $v_k = \hat{v}_{k|k-1} + 1$, $\hat{\boldsymbol{V}}^{(0)}_{k|k} = \hat{\boldsymbol{V}}_{k|k-1}$, factorize covariance matrix $\boldsymbol{P}_{k|k-1}$ using cholesky decomposition

$$\boldsymbol{P}_{k|k-1} = \boldsymbol{S}_{k|k-1}\boldsymbol{S}^T_{k|k-1} \tag{69}$$

Compute the fifth-degree interpolatory cubature points ($l = 1, 2, \ldots, n^2 + 2n + 1$)

$$\boldsymbol{X}_{l,k|k-1} = \boldsymbol{S}_{k|k-1}\boldsymbol{\xi}_l + \hat{\boldsymbol{x}}_{k|k-1} \tag{70}$$

Compute the propagated fifth-degree interpolatory cubature points ($l = 1, 2, \ldots, n^2 + 2n + 1$)

$$\boldsymbol{Z}_{l,k|k-1} = f(\boldsymbol{X}_{l,k|k-1}) \tag{71}$$

Compute the predicted measurement

$$\hat{z}_{k|k-1} = \mathrm{W}_0^{(2,n)}\boldsymbol{Z}_{l,k|k-1} + \mathrm{W}_1^{(2,n)}\sum_{l=2}^{2n+1}\boldsymbol{Z}_{l,k|k-1} + \mathrm{W}_2^{(2,n)}\sum_{l=2n+2}^{2n^2+1}\boldsymbol{Z}_{l,k|k-1} + \mathrm{W}_3^{(2,n)}\sum_{l=2n^2+2}^{2n^2+2n+1}\boldsymbol{Z}_{l,k|k-1} \tag{72}$$

Compute the innovation covariance matrix

$$\begin{aligned}\boldsymbol{P}_{zz,k|k-1} = {} & \mathrm{W}_0^{(2,n)}\boldsymbol{Z}_{l,k|k-1}(\boldsymbol{Z}_{l,k|k-1})^{\mathrm{T}} + \mathrm{W}_1^{(2,n)}\sum_{l=2}^{2n+1}\boldsymbol{Z}_{l,k|k-1}(\boldsymbol{Z}_{l,k|k-1})^{\mathrm{T}} \\ & + \mathrm{W}_2^{(2,n)}\sum_{l=2n+2}^{2n^2+1}\boldsymbol{Z}_{l,k|k-1}(\boldsymbol{Z}_{l,k|k-1})^{\mathrm{T}} + \mathrm{W}_3^{(2,n)}\sum_{l=2n^2+2}^{2n^2+2n+1}\boldsymbol{Z}_{l,k|k-1}(\boldsymbol{Z}_{l,k|k-1})^{\mathrm{T}} \\ & - \hat{z}_{k|k-1}\hat{z}_{k|k-1}^{\mathrm{T}} + \boldsymbol{R}_k\end{aligned} \tag{73}$$

Compute the cross-covariance matrix

$$\begin{aligned}\boldsymbol{P}_{xz,k|k-1} = {} & \mathrm{W}_0^{(2,n)}\boldsymbol{X}_{l,k|k-1}(\boldsymbol{Z}_{l,k|k-1})^{\mathrm{T}} + \mathrm{W}_1^{(2,n)}\sum_{l=2}^{2n+1}\boldsymbol{X}_{l,k|k-1}(\boldsymbol{Z}_{l,k|k-1})^{\mathrm{T}} \\ & + \mathrm{W}_2^{(2,n)}\sum_{l=2n+2}^{2n^2+1}\boldsymbol{X}_{l,k|k-1}(\boldsymbol{Z}_{l,k|k-1})^{\mathrm{T}} + \mathrm{W}_3^{(2,n)}\sum_{l=2n^2+2}^{2n^2+2n+1}\boldsymbol{X}_{l,k|k-1}(\boldsymbol{Z}_{l,k|k-1})^{\mathrm{T}} \\ & - \hat{\boldsymbol{x}}_{k|k-1}\hat{z}_{\mathrm{k|k-1}}^{\mathrm{T}}\end{aligned} \tag{74}$$

Estimate the fading factor λ_k

$$\begin{cases}\boldsymbol{N}_k = \boldsymbol{V}_k - (\boldsymbol{P}_{xz,k|k-1})^{\mathrm{T}}[(\boldsymbol{P}_{k|k-1})^{-1}]^{\mathrm{T}}\boldsymbol{Q}_{k-1}(\boldsymbol{P}_{k|k-1})^{-1} \\ \qquad \times \boldsymbol{P}_{xz,k|k-1} - \beta\boldsymbol{R}_k \\ \boldsymbol{M}_k = \boldsymbol{P}_{zz,k|k-1}^{(i+1)} + \boldsymbol{N}_k - \boldsymbol{V}_k + (\beta - 1)\boldsymbol{R}_k \\ \lambda_k = \max(1, tr[\boldsymbol{N}_k]/tr[\boldsymbol{M}_k])\end{cases} \tag{75}$$

where

$$\boldsymbol{V}_k = \begin{cases}\varepsilon_1\varepsilon_1^{\mathrm{T}}, & k = 1 \\ \dfrac{\rho\boldsymbol{V}_{k-1} + \varepsilon_1\varepsilon_1^{\mathrm{T}}}{1+\rho}, & k \geq 2\end{cases}, \quad \varepsilon_k = z_{k|k} - \hat{z}_{k|k-1}.$$

Estimate the predicted error covariance modified by the fading factor λ_k

$$\boldsymbol{P}'_{k|k-1} = \lambda_k(\boldsymbol{P}_{k|k-1} - \boldsymbol{Q}_{k-1}) + \boldsymbol{Q}_{k-1} \tag{76}$$

By utilizing the predicted state $\hat{\boldsymbol{x}}_{k|k-1}$ and the error covariance $\boldsymbol{P}'_{k|k-1}$ modified by the fading factor λ_k, the modified interpolatory cubature points $\boldsymbol{X}'_{l,k|k-1}$, the modified propagated interpolatory cubature points $\boldsymbol{Z}'_{l,k|k-1}$, the modified predicted measurement $\hat{z}'_{k|k-1}$, the modified measurement innovation covariance without the measurement noise variance $\boldsymbol{P}'_{zz,k||k1}$ and the modified measurement cross-covariance $\boldsymbol{P}'_{xz,k|k-1}$ can be calculated as following equations:

$$\boldsymbol{P}'_{k|k-1} = \boldsymbol{S}_{k|k-1}\boldsymbol{S}_{k|k-1}^{T} \tag{77}$$

$$\boldsymbol{X}'_{l,k|k-1} = \boldsymbol{S}_{k|k-1}\boldsymbol{\xi}_l + \hat{\boldsymbol{x}}_{k|k-1} \tag{78}$$

$$\boldsymbol{Z}'_{l,k|k-1} = f(\boldsymbol{X}'_{l,k|k-1}) \tag{79}$$

$$\hat{z}'_{k|k-1} = \mathrm{W}_0^{(2,n)}\boldsymbol{Z}'_{l,k|k-1} + \mathrm{W}_1^{(2,n)}\sum_{l=2}^{2n+1}\boldsymbol{Z}'_{l,k|k-1} + \mathrm{W}_2^{(2,n)}\sum_{l=2n+2}^{2n^2+1}\boldsymbol{Z}'_{l,k|k-1} + \mathrm{W}_3^{(2,n)}\sum_{l=2n^2+2}^{2n^2+2n+1}\boldsymbol{Z}'_{l,k|k-1} \tag{80}$$

$$\begin{aligned}\boldsymbol{P}'_{zz,k||k1} = {} & \mathrm{W}_0^{(2,n)}\boldsymbol{Z}'_{l,k|k-1}(\boldsymbol{Z}'_{l,k|k-1})^{\mathrm{T}} + \mathrm{W}_1^{(2,n)}\sum_{l=2}^{2n+1}\boldsymbol{Z}'_{l,k|k-1}(\boldsymbol{Z}'_{l,k|k-1})^{\mathrm{T}} \\ & + \mathrm{W}_2^{(2,n)}\sum_{l=2n+2}^{2n^2+1}\boldsymbol{Z}'_{l,k|k-1}(\boldsymbol{Z}'_{l,k|k-1})^{\mathrm{T}} + \mathrm{W}_3^{(2,n)}\sum_{l=2n^2+2}^{2n^2+2n+1}\boldsymbol{Z}'_{l,k|k-1}(\boldsymbol{Z}'_{l,k|k-1})^{\mathrm{T}} \\ & - \hat{z}_{k|k-1}\hat{z}_{k|k-1}^{\mathrm{T}}\end{aligned} \tag{81}$$

$$\begin{aligned}\boldsymbol{P}'_{xz,k|k-1} = {} & \mathrm{W}_0^{(2,n)}\boldsymbol{X}'_{l,k|k-1}(\boldsymbol{Z}'_{l,k|k-1})^{\mathrm{T}} + \mathrm{W}_1^{(2,n)}\sum_{l=2}^{2n+1}\boldsymbol{X}'_{l,k|k-1}(\boldsymbol{Z}'_{l,k|k-1})^{\mathrm{T}} \\ & + \mathrm{W}_2^{(2,n)}\sum_{l=2n+2}^{2n^2+1}\boldsymbol{X}'_{l,k|k-1}(\boldsymbol{Z}'_{l,k|k-1})^{\mathrm{T}} + \mathrm{W}_3^{(2,n)}\sum_{l=2n^2+2}^{2n^2+2n+1}\boldsymbol{X}'_{l,k|k-1}(\boldsymbol{Z}'_{l,k|k-1})^{\mathrm{T}} \\ & - \hat{\boldsymbol{x}}_{k|k-1}(\hat{z}'_{k|k-1})^{\mathrm{T}}\end{aligned} \tag{82}$$

Iterate the following, say N, steps $i = 0, \ldots, N-1$

Compute the modified measurement innovation covariance

$$\boldsymbol{P}_{zz,k||k-1}^{(i+1)} = \boldsymbol{P}'_{zz,k||k-1} + R_k^{(i)}$$

where $R_k^{(i+1)}$ is the equivalent expression of the measurement noise variance matrix, which can be can be estimated by

$$\boldsymbol{R}_k^{(i)} = (\hat{v}_k - m - 1)^{-1}\hat{\boldsymbol{V}}_k^{(i)}$$

Compute the filtering gain

$$K^{(i+1)} = P'_{xz,k|k-1}(P^{(i+1)}_{zz,k||k-1})^{-1} \tag{83}$$

Estimate the updated state

$$\hat{x}^{(i+1)}_{k|k} = \hat{x}_{k|k-1} + K^{(i+1)}(z_k - \hat{z}'_{k|k-1}) \tag{84}$$

Compute the filtering estimation error covariance matrix

$$P^{(i+1)}_{k|k} = P'_{k|k-1} - K^{(i+1)}P^{(i+1)}_{zz,k||k-1}[K^{(i+1)}]^T \tag{85}$$

The parameters of the measurement noise $\hat{V}^{(i+1)}_k$ is updated by as follow

$$\hat{V}^{(i+1)}_k = \hat{V}_{k|k-1} + \int (z_k - h\left(\hat{x}^{(i)}_{k|k}\right))(z_k - h\left(\hat{x}^{(i)}_{k|k}\right))^{\mathrm{T}} \times \mathrm{N}(x_k|\hat{x}^{(i)}_{k|k}, P^{(i)}_{k|k})\mathrm{d}x_k \tag{86}$$

The integral in (86) is determined by the selections of the cubature rule for the Gaussian integral approximations, in this paper, a fifth-degree ICR is used to compute the Gaussian integral.

Set $\hat{V}_{k|k} = \hat{V}^{(N)}_k, \hat{x}_{k|k} = \hat{x}^{(N)}_{k|k}, P_{k|k} = P^{(N)}_{k|k}, R_k = R^{(N)}_k$.

The VB-STICKF combines the advantages of STF, VB and ICKF, which has better filtering accuracy and stronger robustness against model uncertainties and time-varying noise statistics, the proposed VB-STICKF algorithm is summarized in Table 1, and the flow chart of the algorithm is shown in Fig.1.

IV. EXPERIMENT AND DISCUSSION

In this section, the deduced VB-STICKF algorithm is compared with third-degree CKF, third-degree SSRCKF, fifth-degree SSRCKF, fifth-degree CKF, ICKF, VB-STF (STF with VB approximation), third-degree VB-STCKF (third-degree CKF with VB-STF), third-degree VB-STSSRCKF (third-degree SSRCKF with VB-STF) in a target tracking application, where the fixed radar is used to track the maneuvering target with the unknown turn rate, the scenario has been employed to validate the filtering performance of different algorithms.

The nonlinear process equation is formulated as follow

$$x_k = \begin{pmatrix} 1 & \frac{\sin\Omega T}{\Omega} & 0 & -(\frac{1-\cos\Omega T}{\Omega}) & 0 \\ 0 & \cos\Omega T & 0 & -\sin\Omega T & 0 \\ 0 & \frac{1-\cos\Omega T}{\Omega} & 1 & \frac{\sin\Omega T}{\Omega} & 0 \\ 0 & \sin\Omega T & 0 & \cos\Omega T & 0 \\ 0 & 0 & 0 & 0 & 1 \end{pmatrix} \times x_{k-1} + u_{k-1} + w_k \tag{87}$$

where the state $x_k = [x_k, \dot{x}_k, y_k, \dot{y}_k, \Omega]$, x_k and y_k denote positions, $\dot{x}_k$ and $\dot{y}_k$ denote velocities at time k, Ω is uncertain turn rate of the target, u_{k-1} is the system maneuver input, T is the sample time and $T = 1$, simulation time $t = 100s$, the process noise $w_k \sim N(0, \mathbf{Q})$ with the covariance $\mathbf{Q} = diag[q_1\mathbf{M}\ q_1\mathbf{M}\ q_2T]$, $q_1 = 0.01m^2s^{-3}$, $q_2 = 2.625 \times 10^{-5}s^{-3}$, and

$$\mathbf{M} = \begin{bmatrix} T^3/3 & T^2/2 \\ T^2/2 & T \end{bmatrix} \tag{88}$$

Assume the radar locates in the origin of the cartesian coordinate system, the range and the bearing offered by the radar are chosen as the measurement information, thus, the corresponding measurement equation is formulated as

$$y_k = \begin{bmatrix} r_k \\ \theta_k \end{bmatrix} = \begin{pmatrix} \sqrt{x_k^2 + y_k^2} \\ \tan^{-1}(y_k, x_k) \end{pmatrix} + v_k \tag{89}$$

TABLE 1. **VB-STICKF algorithm.**

Initialization: $\hat{x}_{0|0}$, $P_{0|0}$, $\hat{v}_{0|0}$ $\hat{V}_{0|0}$

Prediction:

$\hat{x}_{k|k-1} = \int f\ x_{k-1}\ \mathrm{N}(x_{k-1} | \hat{x}_{k-1|k-1}, P_{k-1|k-1})\mathrm{d}x_{k-1}$

$P_{k|k-1} = \int f\ x_{k-1}\ f^T\ x_{k-1} \times \mathrm{N}(x_{k-1} | \hat{x}_{k-1|k-1}, P_{k-1|k-1}) \times \mathrm{d}x_{k-1} - \hat{x}_{k|k-1}\hat{x}^T_{k|k-1} + Q_{k-1}$

Given $\hat{x}_{k-1|k-1}$, $P_{k-1|k-1}$, compute $\hat{x}_{k|k-1}$, $P_{k|k-1}$ via the time update of ICKF

Given $\hat{v}_{k-1|k-1}$, $\hat{V}_{k-1|k-1}$, compute $\hat{v}_{k|k-1}$, $\hat{V}_{k|k-1}$ via (21)-(22)

Update:

Initialization: $\hat{x}^{(0)}_{k|k} = \hat{x}_{k|k-1}$, $P^{(0)}_{k|k} = P_{k|k-1}$, $\hat{v}_k = \hat{v}_{k|k-1} + 1$, $\hat{V}^{(0)}_k = \hat{V}_{k|k-1}$, and compute the followings:

$\hat{z}_{k|k-1} = \int h\ x_k \times \mathrm{N}(x_k | \hat{x}_{k|k-1}, P_{k|k-1})\mathrm{d}x_k$

$P_{zz,k|k-1} = \int h\ x_k\ h^T\ x_k \times \mathrm{N}(x_k | \hat{x}_{k|k-1}, P_{k|k-1})\mathrm{d}x_k - \hat{z}_{k|k-1}\hat{z}^T_{k|k-1} + R_k$

$P_{xz,k|k-1} = \int x_k h^T\ x_k \times \mathrm{N}(x_k | \hat{x}_{k|k-1}, P_{k|k-1})\mathrm{d}x_k - \hat{x}_{k|k-1}\hat{z}_{k|k-1}$

Given $\hat{x}_{k|k-1}$, $P_{k|k-1}$, compute $\hat{z}_{k|k-1}$, $P_{zz,k|k-1}$, $P_{xz,k|k-1}$ via the measurment update of ICKF

Given $P_{k|k-1}$, $P_{zz,k|k-1}$, $P_{xz,k|k-1}$, compute the fading factor λ_k via (75)

Given λ_k, recompute $P'_{k|k-1}$ with λ_k modification via (76)

Given $P'_{k|k-1}$, recompute $\hat{z}'_{k|k-1}$, $P'_{zz,k|k-1}$, and $P'_{xz,k|k-1}$ via (77)-(82)

For $i = 0 : N-1$

$R^{(i)}_k = (\hat{v}_k - m - 1)^{-1}\hat{V}^{(i)}_k$

$P^{(i+1)}_{zz,k|k-1} = P'_{zz,k|k-1} + R^{(i)}_k$

$K^{(i+1)} = P'_{xz,k|k-1}(P^{(i+1)}_{zz,k\|k-1})^{-1}$

$\hat{x}^{(i+1)}_{k|k} = \hat{x}_{k|k-1} + K^{(i+1)}(z_k - \hat{z}'_{k|k-1})$

$P^{(i+1)}_{k|k} = P'_{k|k-1} - K^{(i+1)}P^{(i+1)}_{zz,k\|k-1}[K^{(i+1)}]^{\mathrm{T}}$

$\hat{V}^{(i+1)}_k = \hat{V}_{k|k-1} + \int (z_k - h\ \hat{x}^{(i)}_{k|k})(z_k - h\ \hat{x}^{(i)}_{k|k})^{\mathrm{T}} \times N(x_k | \hat{x}^{(i)}_{k|k}, P^{(i)}_{k|k})\ \mathrm{d}x_k$

end for

Set $\hat{V}_{k|k} = \hat{V}^{(N)}_k$, $\hat{x}_{k|k} = \hat{x}^{(N)}_{k|k}$, $P_{k|k} = P^{(N)}_{k|k}$, $R_k = R^{(N)}_k$

Output: $\hat{v}_k$, $\hat{V}_{k|k}$, $\hat{x}_{k|k}$, $P_{k|k}$, R_k

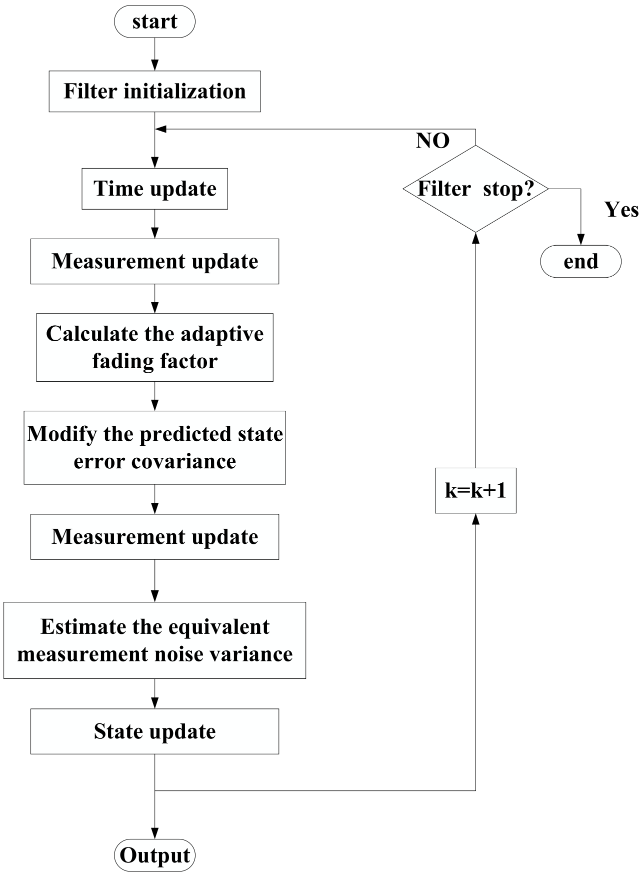

FIGURE 1. VB-STICKF algorithm flow chart.

where $\boldsymbol{v}_k$ is the measurement noise, $\boldsymbol{v}_k \sim N(0, \boldsymbol{R})$ with $\boldsymbol{R} = diag[\sigma_r^2, \sigma_\theta^2]$, where $\sigma_r = 10m, \sigma_\theta = \sqrt{10}mrad$, and the true initial state $\boldsymbol{x}_0$ and the covariance $\boldsymbol{P}_{0|0}$ can be described as

$$\boldsymbol{x}_0 = [1000\text{m}, 300\text{m/s}, 1000\text{m}, 0, -3^\circ/\text{s}] \tag{90}$$

$$\boldsymbol{P}_{0|0} = [100\text{m}^2, 10\text{m}^2/\text{s}^2, 100\text{m}^2, 10\text{m}^2/\text{s}^2, 100\text{mrad}^2/\text{s}^2] \tag{91}$$

In each Monte Carlo run, $\boldsymbol{x}_0$ is generated randomly from the normal distribution $N(\hat{\boldsymbol{x}}_0; \boldsymbol{x}_0, \boldsymbol{P}_{0|0})$, the simulation results are based on 200 Monte Carlo experiments, other parameters are chosen as: $\rho = 0.95$, $\beta = 3.5$, $N = 10$, $\eta = 1 - e^{-4}$.

The root-mean square errors (RMSE) can be selected as the performance metric to access the results of the statistical analysis of different filters, which can be described as

$$\text{RMSE}_{pos}(k) = \sqrt{\frac{1}{M}\sum_{i=1}^{M}(x_k^i - \hat{x}_k^i)^2 + (y_k^i - \hat{y}_k^i)^2} \tag{92}$$

$$\text{RMSE}_{vel}(k) = \sqrt{\frac{1}{M}\sum_{i=1}^{M}(\dot{x}_k^i - \hat{\dot{x}}_k^i)^2 + (\dot{y}_k^i - \hat{\dot{y}}_k^i)^2} \tag{93}$$

$$\text{RMSE}_{\Omega}(k) = \sqrt{\frac{1}{M}\sum_{i=1}^{M}(\Omega_k^i - \hat{\Omega}_k^i)^2} \tag{94}$$

where M is the total number of Monte Carlo simulation, i denotes the ith Monte Carlo run, k denotes the k-th discrete time point of the total simulation time. (x_k^i, y_k^i) and $(\dot{x}_k^i, \dot{y}_k^i)$ denote the true position and velocity, respectively. $(\hat{x}_k^i, \hat{y}_k^i)$ and $(\hat{\dot{x}}_k^i, \hat{\dot{y}}_k^i)$ denote the estimated position and velocity, respectively. Moreover, Ω_k^i and $\hat{\Omega}_k^i$ denote the true and estimated turn rate, respectively. The metrics used to access the results of statistical analysis is the mean and standard deviation of the calculated RMSEs of the position, velocity and turn rate over the time, the mean MRMSE($\chi_{j,k}$) and the standard deviation STDRMSE($\chi_{j,k}$) are given by

$$\text{MRMSE}(\chi_{j,k}) = \frac{1}{N_d}\sum_{k=1}^{N_d}\chi_{j,k} \tag{95}$$

$$\text{STDRMSE}(\chi_{j,k}) = \sqrt{\frac{1}{N_d - 1}\sum_{k=1}^{N_d}(\chi_{j,k} - \hat{\chi}_{j,k})^2} \tag{96}$$

where $N_d = t/T$, which denotes the number of the discrete time, $\chi_{j,k}$ and $\hat{\chi}_{j,k}$ denote the jth element of the true and estimated states of the statistical results at time k.

Target dynamics during the different phases are substantially different, which may be endowed with a variety of uncertainties, including those concerning trajectory loft or depression, thrust profile management, target weight, propellant specific impulse, sensor bias, and external environmental disturbs, etc, many of these uncertainties stem from the uncertainty in the target type [1]–[3]. The performance of the derived VB-STICKF is demonstrated by a target tracking model when the system states suddenly change and the noise covariance matrix is unknown and time-varying, three different scenarios are utilized to verify the filtering accuracy and the robustness of the deduced filtering algorithm.

A. SCENARIO 1

Due to the incomplete prior knowledge and the strong nonlinear motion characteristics of the maneuvering target, the target tracking system may lose the ability to track the target, which seriously affects the real-time property of the tracking system. For example, for anti-radiation missiles, they will quickly change the states of the motion once the beam direction of the radar is measured; Cruise missiles are widely used in military warfare due to the capabilities of small radar cross section and the low-altitude penetration, which make corresponding maneuvers according to the changes in topography and landform; With the rapid development of the warhead maneuvering orbiting technology, the electromagnetic interference technology, and the child bullets, etc, the maneuvering orbits of ballistic missiles will also may cause the target tracking system to lose the tracking ability, even resulting in the divergence of the tracking filter of the ballistic missile defense.

We take the ballistic and space targets (BT) as an example, namely, ballistic missiles, decoys, debris, satellites, projectiles, etc. The entire flight path of a BT is commonly divided into three basic phases: boost, ballistic, and reentry.

The significant forces affects the motion of BTs present in the different phases are boost (thrust, gravity, and aerodynamic), coast (gravity), and reentry (aerodynamic and gravity). However, the motion of a BT can't be predetermined accurately. In this section, we considers a target maneuver tracking scenario where the target make a sudden motion [37], [38]. To test the robustness of the proposed VB-STICKF, we assume that the target makes an uniform motion without the maneuver during the first 20s, that is, $u_{k-1} = [0\text{m}, 0\text{m/s}, 0\text{m}, 0\text{m/s}, 0^{\circ}/\text{s}]$, then, it makes a maneuver with $u_{k-1} = [0\text{m}, 5\text{m/s}, 0\text{m}, -5\text{m/s}, 0.2^{\circ}/\text{s}]$ in the interval of 20–30s, the scenario is executed to compare the performance of VB-STICKF and others filtering algorithms listed in the paper, the RMSEs on the position estimation, velocity estimation, and the turn rate estimation of different filtering algorithms are shown in Figs. 2-4, respectively, the curve of the adaptive fading factor of the proposed VB-STCKF algorithm is shown in Fig. 5

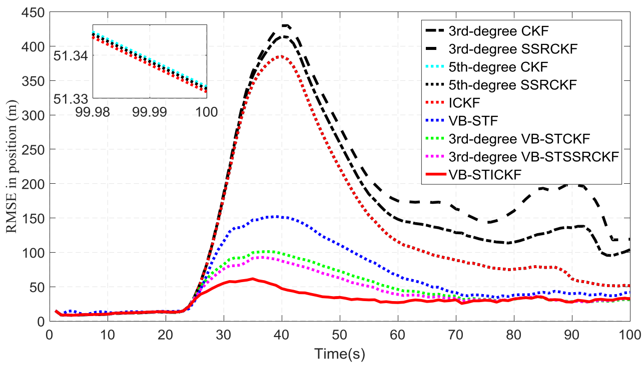

FIGURE 2. Root mean square error (RMSE) of the estimated position.

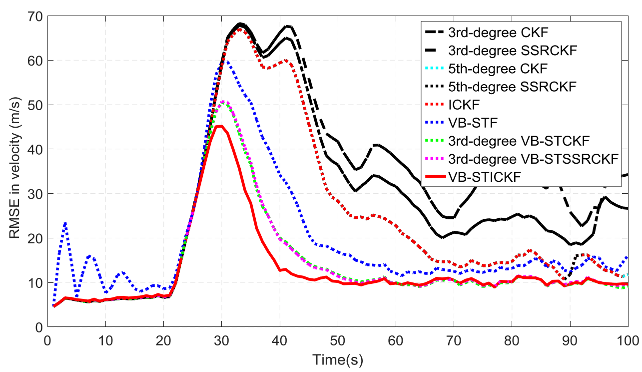

FIGURE 3. RMSE of the estimated velocity.

As a whole, we can see from the curves of calculated RMSEs of the position, velocity, and turn rate that all the filtering methods exhibit a more or less fluctuation or even diverge due to a mismatch model, which is mainly induced by the fact that the target make a sudden maneuver, resulting in the established model does not match the actual system. As can be seen from Fig. 2, it denotes the calculated RMSEs of the position. Nine different methods show an indiscernibly close performance when the target makes an uniform motion without any maneuver during the first 20s. Once the maneuver begins at time t = 21s, we can conclude from Fig. 2 that the VB-STF, the third-degree VB-STCKF, the third-degree VB-STSSRCKF, and the proposed VB-STICKF all have the ability to converge quickly, that is, the nonlinear filters with STF algorithm show slighter fluctuation and faster convergence rate than the filtering methods without the fading factor modification. Here we give a deep analysis and description.

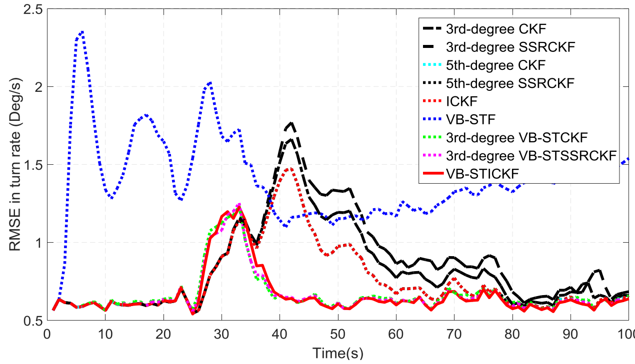

FIGURE 4. RMSE of the estimated turn rate.

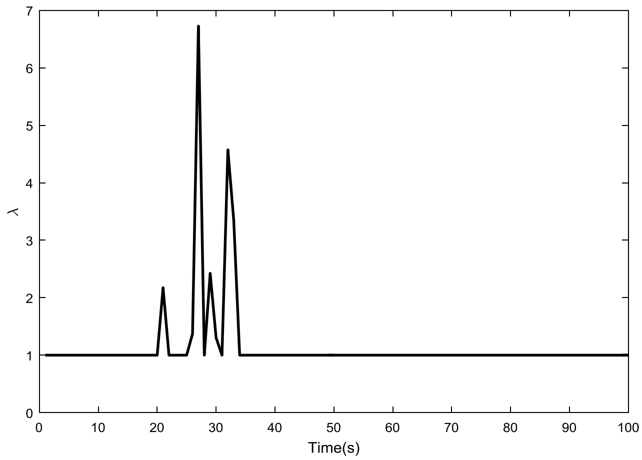

FIGURE 5. The adaptive fading factor.

According to the analysis of section II, STF algorithm is based on the orthogonality principle, which has uncorrelated Gaussian white noise-like properties. It means that all valid information in the residual sequence have been extracted by the filter. When the target make a sudden maneuver, that is, the established model does not exactly match the actual system, which causes the abnormal change in one-step state prediction $\hat{\boldsymbol{x}}_{k|k-1} = \boldsymbol{f}(\hat{\boldsymbol{x}}_{k-1|k-1})$ due to the function $\boldsymbol{f}(\bullet)$, the residual sequences $\boldsymbol{\gamma}_k = z_{k|k} - \boldsymbol{h}\left(\hat{\boldsymbol{x}}_{k|k-1}\right)$ also change, the residual sequences may be not mutually orthogonal. By introducing the STF and modifying the predicted state error covariance matrix by an adaptive fading factor, thus the filtering gain could be adaptively adjusted on-line, the residual sequence is forced to be orthogonal, which has effectively refined the poor filtering performance caused by the uncertain factors. Relying on the fading factor, the STF algorithm makes full use of the effective information in the residual sequence and shows better robustness to resist the uncertainties of the system model. It can be clearly seen from Fig.5 that the VB-STICKF produces a fading factor greater than 1 after the target make a sudden maneuver, and then the fading factor decreases until it drops to 1, thus ensuring strong tracking ability to track the target state and avoiding over-adjustment of the filtering gain. The results show the effectiveness of the STF algorithm and the superiority of the proposed VB-STICKF algorithm. When there is no large model mismatch, the fading factor can be automatically taken as 1, just like the only nonlinear filter, it does not affect the estimation accuracy of the system state.

In addition, we can see from Figs. 2 that the proposed VB-STICKF shows better filtering accuracy and faster convergence rate compared with other algorithms. We can also see from Fig.2 that curves of the fifth-degree CKF, the fifth-degree SSRCKF and ICKF are nearly overlapped, the local magnification processing is performed to analyze and compare three fifth-degree filtering methods, ICKF has slightly better filtering performance. Similarly to the RMSEs in position, Figs. 3 and 4 show RMSEs of the velocity and the turn rate of different filtering algorithms in an interval of 0–100s, the proposed VB-STICKF also has better estimation accuracy and faster convergence speed than other filtering algorithms.

Now we mainly focus on the analysis of VB-STF algorithm, although it inherits the advantages of the strong robustness of STF algorithm, it can be seen from Fig. 2 -Fig.4 that VB-STF still show much larger fluctuation than other nonlinear filters with STF algorithm, such as the third-degree VB-STCKF, the third-degree VB-STSSRCKF, and the proposed VB-STICKF. This is because that the STF is based on theoretical frame of EKF, nevertheless, the derivation of EKF is based on the first-order Taylor series approximation for nonlinear functions, which can only achieve first-order accuracy induced by introducing high-order truncation errors, so it has worse filtering accuracy than other GA filters for the maneuvering target tracking problem, especially as shown in Fig.4. Furthermore, as shown in Fig.2- Fig.3, owing to the fact that VB-STF owns the strong robustness of STF algorithm, although VB-STF can only obtain first-order accuracy for nonlinear functions, it still has the better ability to track the maneuvering target than other nonlinear filters without STF algorithm. To quantitatively describe the tracking performance, the mean and the standard deviation of the calculated RMSEs of the position, velocity and turn rate over the time interval in Figs. 2-4 are given in Table 2 for comparison.

The difference of the fluctuation of RMSEs over time can be also reflected on quantitative comparison of the filtering results. We take ICKF and VB-STSSRCKF as the representative methods for comparison. Gaussian approximate filter used in the paper is ICKF, 3rd-degree VB-STSSRCKF with known measurement noise covariance mentioned in the paper can be seen as STSSRCKF, which is proposed for maneuvering target tracking when the target make a sudden maneuver in [22], the algorithm combines STF and SSRCKF. The proposed VB-STICKF is compared with ICKF and 3rd-degree VB-STSSRCKF and the filtering results are described qualitatively. The MRMSEs of the position, the velocity and the turn rate from the proposed filter are respectively reduced by 74.49%, 44.75% and 12.38% as compared with the existing ICKF, in addition, the MRMSEs of the position, velocity and turn rate from the proposed filter are respectively reduced by 24.68%, 9.05% and 0.15% as compared with the existing 3rd-degree VB-STSSRCKF, the quantitative comparison of the results show the effectiveness of the STF algorithm and the superiority of the proposed VB-STICKF algorithm.

TABLE 2. Performance comparison when the system states change.

Filter	position		velocity		turn rate	
	mean	std	mean	std	mean	std
3rd-degree CKF	145.6581	116.6392	28.4254	18.4865	0.81971	0.2672
3rd-degree SSRCKF	167.6340	121.0890	32.6458	18.6972	0.87055	0.29685
5th-degree CKF	118.5067	112.1314	23.2388	18.3285	0.75664	0.22238
5th-degree SSRCKF	118.5062	112.1313	23.2387	18.3285	0.75663	0.22238
ICKF	118.5060	112.1320	23.2386	18.3285	0.75663	0.22238
VB-STF	60.6545	45.7494	19.2266	13.1889	1.4009	0.28425
3rd-degree VB-STCKF	43.7326	28.7600	14.0402	10.914	0.66961	0.14694
3rd-degree VB-STSSR CKF	40.1302	24.8583	14.116	10.9864	0.66395	0.13784
VB-STICKF	**30.2280**	**13.4400**	**12.8392**	**9.1324**	**0.66298**	**0.13777**

As a whole, it can be seen from Table 2 that the proposed VB-STICKF has significantly smaller MRMSEs and STDRMSEs than other filtering methods, which indicates the slighter fluctuation and the faster convergence rate of the proposed filter as compared with the existing methods. The same conclusion can be obtained that the proposed VB-STICKF outperforms the other methods considerably, which has the highest estimation accuracy and the fastest convergence rate of the position estimation, the velocity estimation and the turn rate estimation, suggesting that VB-STICKF algorithm not only has the robustness of STF against model uncertainties, but also inherits the ability to better to process the nonlinear target tracking problem.

B. SCENARIO 2

In the practical application, because of the complex battlefield environment and the changeable target motion characteristics, the uncertainties of the environment and the model parameters can produce unpredictable modeling errors, resulting in the uncertainties of the target itself, which is characterized by the performance of the uncertain motion as well as the unknown or time-varying process noise statistical characteristics, that is, the process noise statistical characteristics during the different phases differ significantly in general. The process noise is generally assumed to be zero-mean Gaussian white noise distribution, which obviously does not accord with the actual situation. In this section, in order to test the robustness of the proposed VB-STICKF, we deliberately make the process noise covariance matrix to satisfy an inaccurate and time-varying form. The initial parameters have been defined as description above, the true process noise covariance $\mathbf{Q}'$ can be described as

$$\mathbf{Q}' = (10 + 2.5\cos(\frac{\pi k}{t}))\mathbf{Q} \tag{97}$$

where $\mathbf{Q} = diag[q_1\mathbf{M}q_1\ \mathbf{M}q_2\ T]$ is the nominal covariance matrix in the interval of 0–100s, t is simulation time, k denotes time variable. the scenario is executed to examine the performance of the derived VB-STICKF and other filtering algorithms, the RMSEs on the position estimation, velocity estimation, and turn rate estimation of different filtering algorithms are shown in Figs. 6-8, respectively, the curve of the adaptive fading factor of the proposed VB-STCKF algorithm in the scenario is shown in Fig. 9

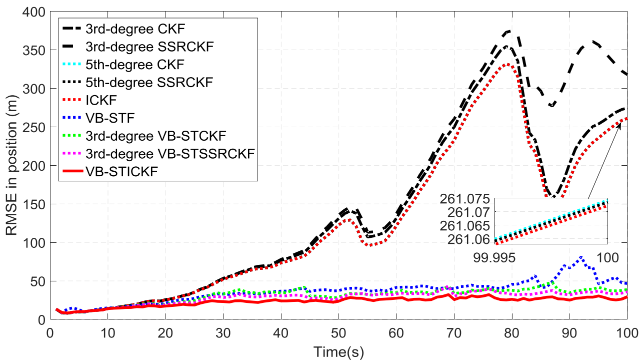

FIGURE 6. RMSE of the estimated position.

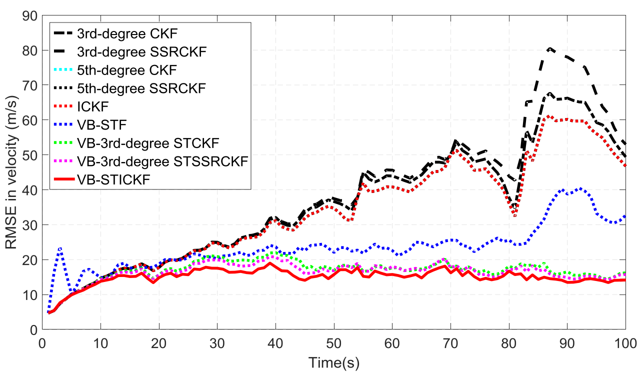

FIGURE 7. RMSE of the estimated velocity.

Overall, we can see from Figs. 6-8 that the third-degree CKF, the fifth-degree CKF, the third-degree SSRCKF, the fifth-degree SSRCKF and ICKF exhibit larger fluctuation than other nonlinear filtering methods with the fading factor modification due to a mismatch model, which is mainly

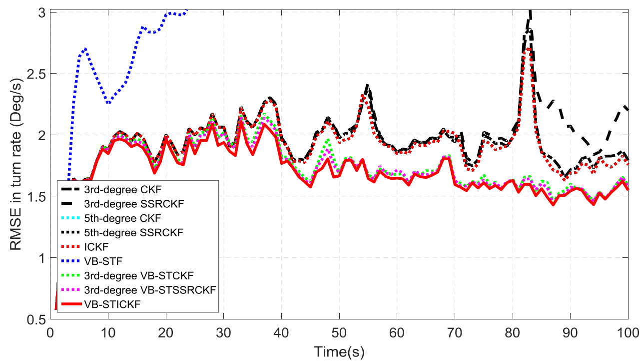

FIGURE 8. RMSE of the estimated turn rate.

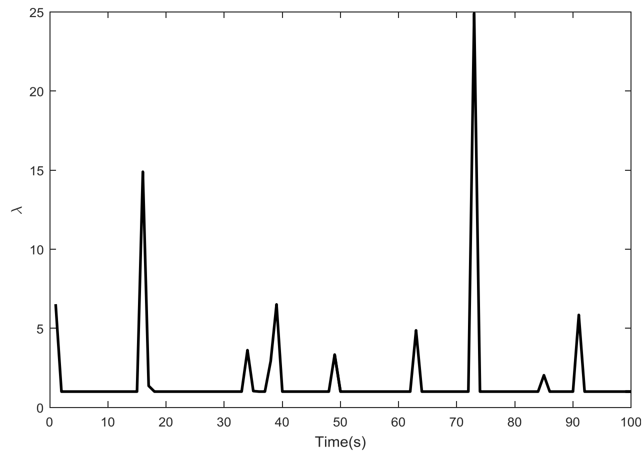

FIGURE 9. The adaptive fading factor.

induced by the time-varying process noise covariance, resulting in the established model does not match the actual system. It is obviously that VB-STF, third-degree VB-STCKF, third-degree VB-STSSRCKF, and the proposed VB-STICKF all have strong robustness against the time-varying process noise and better estimation accuracy, which is mainly induced by the fact that the adaptive fading factor from STF is added to the equations of the measurement update, thus the filtering gain matrix could be adaptively adjusted on-line, and the poor performance resulted by the process noise uncertainty could be effectively prevented, the detailed explanations can be see in scenario 1 and the derivation of STF. In addition, we can conclude that the proposed VB-STICKF shows better estimation accuracy and faster convergence speed among all listed filers in the simulation. Now we mainly focus on the analysis of VB-STF algorithm, which is similar to the scenario 1. Although it inherits the advantages of the strong robustness of STF algorithm, it can be seen from Fig. 6 -Fig.7 that VB-STF still show much larger fluctuation than other nonlinear filters with the fading factor modification, what's more, as shown in Fig.8, the curve of the calculated RMSEs of the turn rate is divergent. This is because that the VB-STF can only achieve first-order accuracy induced by introducing high-order truncation errors. As shown in the Fig. 9, VB-STICKF produces a fading factor greater than 1 when the process noise covariance matrix is unknown and time-varying, and then the fading factor decreases until it drops to 1, the algorithm makes full use of the effective information in the residual sequence and shows better robustness to resist the unknown and time-varying process noise statistics. To quantitatively describe the tracking performance, the mean and the standard deviation of the calculated RMSEs of the position, velocity and turn rate over time interval in Figs. 6-8 are given in Table 3 for comparison.

TABLE 3. Performance comparison when the process noise vary.

Filter	position		velocity		turn rate	
	mean	std	mean	std	mean	std
3rd-degree CKF	134.7227	104.5978	35.9724	16.5978	1.9304	0.2513
3rd-degree SSRCKF	155.749	127.0091	38.3789	19.7396	1.9876	0.2639
5th-degree CKF	125.8844	97.2803	34.0608	15.0152	1.9079	0.2462
5th-degree SSRCKF	125.8841	97.2799	34.0608	15.0151	1.9078	0.2462
ICKF	125.8838	97.2794	34.0607	15.015	1.9078	0.2462
VB-STF	36.5947	14.3965	23.5869	6.3085	3.9258	0.9874
3rd-degree VB-STCKF	31.0965	9.6247	16.975	3.0716	1.7342	0.2187
3rd-degree VB-STSSR CKF	28.2972	8.1896	16.4146	2.8539	1.7237	0.2139
VB-STICKF	**23.2282**	**5.6962**	**15.0212**	**2.3383**	**1.6964**	**0.2061**

The difference of the fluctuation of RMSEs over time can be reflected on quantitative comparison of the filtering results. We also take ICKF and VB-STSSRCKF as the representative methods for comparison since that Gaussian approximate filter used in the paper is ICKF and the 3rd-degree VB-STSSRCKF is proposed in the open literatures for maneuvering target tracking. The MRMSEs of the position, the velocity and the turn rate from the proposed filter are respectively reduced by 81.55%, 55.90% and 11.08% as compared with the existing ICKF, in addition, the MRMSEs of the position, velocity and turn rate from the proposed filter are respectively reduced by 17.91%, 8.49% and 1.55% as compared with the existing 3rd-degree VB-STSSRCKF, the quantitative comparison of the results also show the effectiveness of the STF algorithm and the superiority of the proposed algorithm.

As a whole, it can be seen from Table 3 that the proposed VB-STICKF has significantly smaller MRMSEs and STDRMSEs than other filtering methods, which means the proposed VB-STICKF has slighter fluctuation and faster convergence rate than the existing methods. The same conclusion can be also obtained that the proposed VB-STICKF outperforms the other methods considerably, which has the best performance in terms of the filtering accuracy and the convergence rate among all listed filers in the simulation.

C. SCENARIO 3

For the problem of the maneuvering target tracking, we should not only consider the uncertainties of the target itself, but also take the uncertainty of the tracking system into consideration, that is, the measured errors of the target tracking means [39]. With the complex battlefield environment increasingly and the continuous development of stealth technology, more and more attention has been paid to the maneuvering target tracking in complex environments. For example, various kinds of fighters, drones, and missiles can not only take off and attack in the dark, but also carry out tasks under extreme conditions such as high winds, heavy rains, and low temperatures, resulting in the uncertainties of the tracking system, which is characterized by uncertain or time-varying measurement noise statistical characteristics, that is, the measurement noise statistical characteristics during the different phases differ significantly in general. This is because that the accuracy of measurement information is easily disturbed by the external environment as well as the sensor errors, what's more, the uncertainty of measurement information may be caused by the clutter, false alarms and the effect of the adjacent targets [40]. The measurement noise is generally assumed to be zero-mean Gaussian white noise distribution, which obviously does not accord with the actual situation. In this section, we deliberately make the measurement noise covariance matrix to follow an time-varying form to test and compare the robustness of the proposed VB-STICKF. The initial parameters have been defined as description above, the true measurement noise covariance $\boldsymbol{R}'$ can be formulated as

$$\boldsymbol{R}' = (10 + 0.5\cos(\frac{\pi k}{t}))\boldsymbol{R} \tag{98}$$

where $\boldsymbol{R} = diag[\sigma_r^2, \sigma_\theta^2]$ is the nominal covariance matrix in the interval of 0–100s, t is simulation time, k denotes time variable. the scenario is executed to examine the performance of the deduced VB-STICKF and other filtering algorithms, the RMSEs on the position estimation, velocity estimation, and turn rate estimation of different filtering algorithms are shown in Figs. 10-12, respectively.

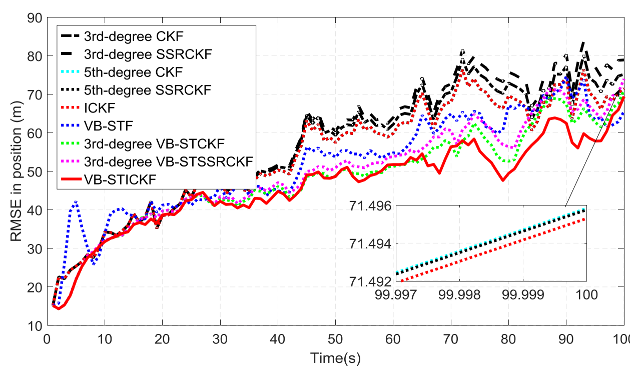

FIGURE 10. RMSE of the estimated position.

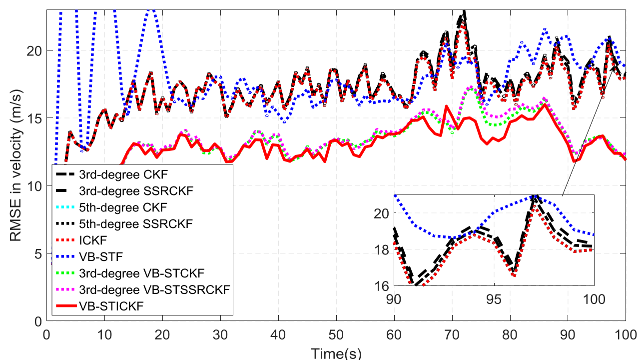

FIGURE 11. RMSE of the estimated velocity.

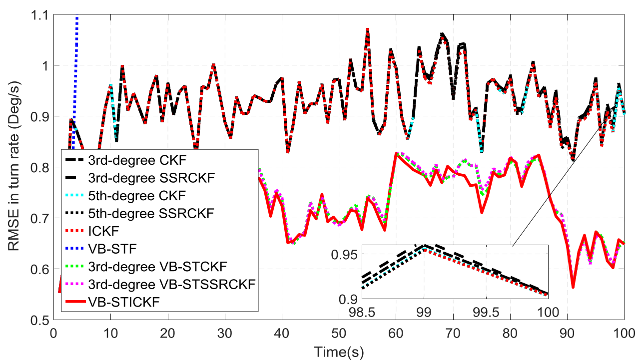

FIGURE 12. RMSE of the estimated turn rate.

As can be seen from Figs. 10-12, it is obviously that the third-degree CKF, the fifth-degree CKF, the third-degree SSRCKF, the fifth-degree SSRCKF and ICKF exhibit much larger errors as compared with the filtering methods with variational Bayesian (VB) estimation when the measurement noise covariance is time-varying. This is because that proposed VB based strong tracking Gaussian approximate filter can effectively estimate the state along with the time-varying measurement noise for the nonlinear systems, VB approximation is utilized to estimate the measurement noise covariance and the GA filter is exploited to deal with the nonlinearities, so the filtering methods with VB estimation have strong robustness against the time-varying measurement noise and better estimation accuracy, the detailed explanations can be seen in the derivation of VB approximation algorithm for GA filter of the section II. It is worth mentioning that the calculated RMSE from VB-STF shows much larger fluctuation and error than other GA filters with VB estimation in Fig. 10-Fig.11, in addition, as shown in Fig.12, the curve of the calculated RMSE of the turn rate is even divergent, this is mainly induced by the fact that VB-STF is based on theoretical frame of EKF, which has poor filtering accuracy in estimating the states of the strongly nonlinear system since that EKF only can achieve the first-order Taylor series approximation for nonlinear functions. We can also conclude from Figs.10-12 that the curves of the fifth-degree Gaussian filtering based algorithms are nearly overlapped, the local magnification processing is performed to analyze the estimation accuracy, the conclusion can be obtained that ICKF has slightly better filtering performance to process the nonlinear problems. In addition, we can see from Figs. 10-12 that the proposed VB-STICKF shows the best performance in terms of the filtering accuracy and the convergence speed among all listed filers in the simulation. To quantitatively describe the tracking performance, the mean and the standard deviation of the calculated RMSEs of the position, velocity and turn rate over the time interval in Figs. 10-12 are given in Table 4 for comparison.

From Table 4, the same conclusion can be obtained that the proposed VB-STICKF outperforms the other methods considerably, which has smaller MRMSEs and STDRMSEs than other filtering methods, suggesting that the VB-STICKF algorithm not only has the ability to better to process the nonlinear target tracking model, but also can effectively estimate the time-varying measurement noise. We take ICKF as the representative method for comparison since that GA filter used in the paper is ICKF, the MRMSEs of the position, the velocity and the turn rate from the proposed filter are respectively reduced by 14.70%, 23.84% and 22.09% as compared with the existing ICKF, the STDRMSEs of the position, the velocity and the turn rate from the proposed filter are respectively reduced by 24.20%, 26.07% and 22.60% as compared with the existing ICKF. The results demonstrate the superiority of the deduced variational Bayesian based strong tracking Gaussian filtering algorithm.

TABLE 4. Performance comparison when the measurement noise vary.

Filter	position		velocity		turn rate	
	mean	std	mean	std	mean	std
3rd-degree CKF	56.2047	16.3662	17.0043	2.6018	0.9203	0.0778
3rd-degree SSRCKF	57.6088	17.5361	17.1271	2.6613	0.9219	0.0782
5th-degree CKF	54.4977	15.0576	16.8509	2.5018	0.9184	0.0771
5th-degree SSRCKF	54.4977	15.0576	16.8508	2.5019	0.9184	0.0771
ICKF	54.497	15.0569	16.8507	2.5018	0.9184	0.0770
VB-STF	52.0801	12.8072	18.3582	3.495	1.9583	0.3746
3rd-degree VB-STCKF	48.18	12.691	13.1767	2.0359	0.7197	0.0613
3rd-degree VB-STSSR CKF	49.7988	13.7004	13.291	2.0992	0.7210	0.0625
VB-STICKF	**46.4847**	**11.4134**	**12.8329**	**1.8495**	**0.7155**	**0.0596**

GA filters used in the paper is ICKF, the computational complexity is almost proportional to the number of sample points, which are listed in Table 5.

We can see from Table 5 that the number of VB-STICKF is 61, the time consumption is acceptable compared with

TABLE 5. Number of sample points of different algorithms.

Algorithms	Number of sample points
3rd-degree CKF	10
3rd-degree SSRCKF	12
5th-degree CKF	51
5th-degree SSRCKF	43
ICKF	61
VB-STF	-
3rd-degree VB-STCKF	10
3rd-degree VB-STSSRCKF	12
VB-STICKF	61

other filters. From the results of the simulation, we can conclude that the proposed VB-STISCKF shows the best performance considering the balance between the filtering performance and the computational cost.

V. CONCLUSION

In this work, we have concentrated on handling the problem of the maneuvering target tracking models with abrupt state changes and time-varying process and measurement noise, a novel variational bayesian based strong tracking interpolatory cubature kalman filter (VB-STICKF) is deduced. The algorithm has provided the linear equivalent describe of STF and could deal with the normal nonlinear system, a fifth-degree interpolatory cubature rule is introduced to numerically compute the numerical integrals. What's more, based on the frame of recursive Bayesian estimation, the measurement noise can be estimated online by the deduced variational Bayesian approximation algorithm, which can be utilized to estimate the measurement noise along with the states for the nonlinear models. Simulation results illustrate that proposed VB-STICKF algorithm not only has better estimation accuracy and filtering performance compared with other filtering algorithms, but also has better robustness to resist the model uncertainty and the time-varying process and measurement noise.

REFERENCES

[1] H. Zhang, J. Xie, J. Ge, W. Lu, and B. Zong, "Adaptive strong tracking square-root cubature Kalman filter for maneuvering aircraft tracking," *IEEE Access*, vol. 6, pp. 10052–10061, 2018.

[2] X. R. Li and V. P. Jilkov, "Survey of maneuvering target tracking. Part I. Dynamic models," *IEEE Trans. Aerosp. Electron. Syst.*, vol. 39, no. 4, pp. 1333–1364, Oct. 2003.

[3] X. R. Li and V. P. Jilkov, "Survey of maneuvering target tracking. Part II: Motion models of ballistic and space targets," *IEEE Trans. Aerosp. Electron. Syst.*, vol. 46, no. 1, pp. 96–119, Jan. 2010.

[4] H. Liu and W. Wu, "Strong tracking spherical simplex-radial cubature Kalman filter for maneuvering target tracking," *Sensors*, vol. 17, no. 4, pp. 741–753, Apr. 2017.

[5] H. Liu and W. Wu, "Interacting multiple model (IMM) fifth-degree spherical simplex-radial cubature Kalman filter for maneuvering target tracking," *Sensors*, vol. 17, no. 6, pp. 1374–1385, Jun. 2017.

[6] M. Yu, L. Gong, H. Oh, W.-H. Chen, and J. Chambers, "Multiple model ballistic missile tracking with state-dependent transitions and Gaussian particle filtering," *IEEE Trans. Aerosp. Electron. Syst.*, vol. 54, no. 3, pp. 1066–1081, Jun. 2018.

[7] X. Wang, Y. Liang, Q. Pan, and C. Zhao, "Gaussian filter for nonlinear systems with one-step randomly delayed measurements," *Automatica*, vol. 49, no. 4, pp. 976–986, Apr. 2013.

[8] X. Wang, Y. Liang, Q. Pan, and H. Huang, "Gaussian/Gaussian-mixture filters for non-linear stochastic systems with delayed states," *IET Control Theory Appl.*, vol. 8, no. 11, pp. 996–1008, Jul. 2014.

[9] I. Arasaratnam and S. Haykin, "Cubature Kalman filters," *IEEE Trans. Autom. Control*, vol. 54, no. 6, pp. 1254–1269, Jun. 2009.

[10] B. Jia, M. Xin, and Y. Cheng, "High-degree cubature Kalman filter," *Automatica*, vol. 49, no. 2, pp. 510–518, Feb. 2013.

[11] X.-C. Zhang and Y.-L. Teng, "A new derivation of the cubature Kalman filters," *Asian J. Control*, vol. 16, no. 5, pp. 1501–1510, Sep. 2014.

[12] S. Wang, J. Feng, and C. K. Tse, "Spherical simplex-radial cubature Kalman filter," *IEEE Signal Process. Lett.*, vol. 21, no. 1, pp. 43–46, Jan. 2014.

[13] Y. Zhang, Y. Huang, N. Li, and L. Zhao, "Embedded cubature Kalman filter with adaptive setting of free parameter," *Signal Process.*, vol. 114, no. 3, pp. 112–116, Sep. 2015.

[14] Y.-L. Huang, Y.-G. Zhang, and Z.-M. Wu, "A high order unscented Kalman filtering method," *Acta Automat. Sinica*, vol. 40, no. 5, pp. 838–848, May 2014.

[15] Y. Zhang, Y. Huang, N. Li, and L. Zhao, "Interpolatory cubature Kalman filters," *IET Control Theory Appl.*, vol. 9, no. 11, pp. 1731–1739, Jul. 2015.

[16] S. Bhaumik and Swati, "Cubature quadrature Kalman filter," *IET Signal Process.*, vol. 7, no. 7, pp. 533–541, Sep. 2013.

[17] A. K. Singh and S. Bhaumik, "Higher degree cubature quadrature Kalman filter," *Int. J. Control Autom. Syst.*, vol. 13, no. 5, pp. 1097–1105, Oct. 2015.

[18] D. Meng, L. Miao, H. Shao, and J. Shen, "A seventh-degree cubature Kalman filter," *Asian J. Control*, vol. 20, no. 1, pp. 250–262, Jan. 2018.

[19] D. H. Zhou and P. M. Frank, "Strong tracking filtering of nonlinear time-varying stochastic systems with coloured noise: Application to parameter estimation and empirical robustness analysis," *Int. J. Control*, vol. 65, no. 2, pp. 295–307, Oct. 1996.

[20] L. Wang, L. Wu, Y. Guan, and G. Wang, "Online sensor fault detection based on an improved strong tracking filter," *Sensors*, vol. 15, no. 2, pp. 4578–4591, Feb. 2015.

[21] Y. Geng and J. Wang, "Adaptive estimation of multiple fading factors in Kalman filter for navigation applications," *GPS Solutions*, vol. 12, no. 4, pp. 273–279, Nov. 2007.

[22] Q. Xia, M. Rao, Y. Ying, and X. Shen, "Adaptive fading Kalman filter with an application," *Automatica*, vol. 30, no. 8, pp. 1333–1338, Aug. 1994.

[23] X.-X. Wang, L. Zhao, Q.-X. Xia, and Y. Hao, "Strong tracking filter based on unscented transformation," *Control Decis.*, vol. 25, no. 10, pp. 1063–1068, Jul. 2010.

[24] N. Cui, L. Zhang, X. Wang, F. Yang, and B. Lu, "Application of adaptive high-degree cubature Kalman filter in target tracking," *Chin. J. Aeronaut.*, vol. 36, no. 12, pp. 3885–3895, Dec. 2015.

[25] R. K. Mehra, "Approaches to adaptive filtering," *IEEE Trans. Autom. Control*, vol. 17, no. 5, pp. 693–698, Oct. 1972.

[26] X. Gao, D. You, and S. Katayama, "Seam tracking monitoring based on adaptive Kalman filter embedded Elman neural network during high-power fiber laser welding," *IEEE Trans. Ind. Electron.*, vol. 59, no. 11, pp. 4315–4325, Nov. 2012.

[27] M. Karasalo and X. Hu, "An optimization approach to adaptive Kalman filtering," *Automatica*, vol. 47, no. 8, pp. 1785–1793, Aug. 2011.

[28] S. Sarkka and A. Nummenmaa, "Recursive noise adaptive Kalman filtering by variational Bayesian approximations," *IEEE Trans. Autom. Control*, vol. 54, no. 3, pp. 596–600, Mar. 2009.

[29] S. Särkkä and J. Hartikainen. (Feb. 2013). "Variational Bayesian adaptation of noise covariances in non-linear Kalman filtering." [Online]. Available: https://arxiv.org/abs/1302.0681

[30] Z.-Y. Miao, Y.-L. Lv, D.-J. Xu, F. Shen, and S.-W. Pang, "Analysis of a variational Bayesian adaptive cubature Kalman filter tracking loop for high dynamic conditions," *GPS Solutions*, vol. 21, no. 1, pp. 111–122, Jan. 2017.

[31] S. Särkkä and J. Hartikainen, "Non-linear noise adaptive Kalman filtering via variational Bayes," in *Proc. IEEE Int. Workshop Mach. Learn. Signal Process.*, Sep. 2013, pp. 1–6.

[32] P. Dong, Z. Jing, H. Leung, and K. Shen, "Variational Bayesian adaptive cubature information filter based on Wishart distribution," *IEEE Trans. Autom. Control*, vol. 62, no. 11, pp. 6051–6057, Nov. 2017.
[33] Y.-L. Huang, Y.-G. Zhang, Z.-M. Wu, N. Li, and J. Chambers, "A novel adaptive Kalman filter with inaccurate process and measurement noise covariance matrices," *IEEE Trans. Autom. Control*, vol. 63, no. 2, pp. 594–601, Feb. 2018.
[34] Y. Wu, D. Hu, M. Wu, and X. Hu, "A numerical-integration perspective on Gaussian filters," *IEEE Trans. Signal Process.*, vol. 54, no. 8, pp. 2910–2921, Aug. 2006.
[35] P. S. Maybeck, *Stochastic Models, Estimation and Control*. New York, NY, USA: Academic, 1979.
[36] D.-H. Zhou, Y.-G. Xi, and Z.-J. Zhang, "A suboptimal multiple fading extended Kalman filter," *Acta Astronaut. Sinica*, vol. 17, no. 6, pp. 689–695, Nov. 1991.
[37] K. Lu, R. Zhou, and J. Zhang, "Approximate Chernoff fusion of Gaussian mixtures for ballistic target tracking in the re-entry phase," *Aerosp. Sci. Technol.*, vol. 61, pp. 21–28, Feb. 2017.
[38] N. Wu, L. Chen, Y. Lei, and F. Meng, "Adaptive estimation algorithm of boost-phase trajectory using binary asynchronous observation," *Proc. Ins. Mech. Eng. G, J. Aerosp. Eng.*, vol. 230, no. 14, pp. 2661–2672, Dec. 2016.
[39] X. He, Y. Bi, and Y. Guo, "Target tracking algorithm of ballistic missile in boost phase based on ground-based radar systems," *J. Inf. Comput. Sci.*, vol. 12, no. 2, pp. 855–864, Jan. 2015.
[40] M. Yu, W.-H. Chen, and J. Chambers, "State dependent multiple model-based particle filtering for ballistic missile tracking in a low-observable environment," *Aerosp. Sci. Technol.*, vol. 67, pp. 144–154, Aug. 2017.

JIAN WANG received the M.S. degree from Harbin Engineering University, Harbin, China, in 2016. He is currently pursuing the Ph.D. degree in instrument science and technology with Southeast University, Nanjing, China.

His current research interests include signal processing, information fusion, the strapdown inertial navigation, initial alignment, and SINS/USBL integration navigation.

TAO ZHANG received the Ph.D. degree in navigation, guidance, and control from Southeast University, Nanjing, China, in 2008.

He is currently an Associate Professor with the School of Instrument Science and Engineering, Southeast University. His current research interests include the ship's acoustic navigation system, long base line, ultra short base line, inertial navigation, and SINS/USBL integration navigation.

XIANG XU received the M.S. degree from Harbin Engineering University, Harbin, China, in 2014. He is currently pursuing the Ph.D. degree in instrument science and technology with Southeast University, Nanjing, China.

His current research interests include strapdown inertial navigation, initial alignment, integrated navigation, information fusion, and system integration.

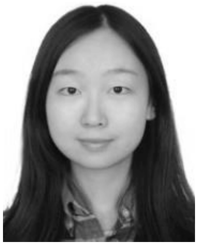

YAO LI received the Ph.D. degree in navigation, guidance, and control from Southeast University, Nanjing, China, in 2012.

She is currently a Lecturer with the School of Instrument Science and Engineering, Southeast University. Her current research interests include inertial navigation, initial alignment, integrated navigation, information fusion, and system integration.